Synthesis, Biological Activity, and Three-Dimensional Quantitative Structure−Activity Relationship Model for a Series of Benzo[*c*]quinolizin-3-ones, Nonsteroidal Inhibitors of Human Steroid 5α-Reductase 1

Ernesto G. Occhiato,[†] Alessandro Ferrali,[†] Gloria Menchi,[†] Antonio Guarna,*[,†] Giovanna Danza,[‡] Alessandra Comerci,[‡] Rosa Mancina,[‡] Mario Serio,[‡] Gianni Garotta,[§] Andrea Cavalli,*[,#] Marco De Vivo,[#] and Maurizio Recanatini[#]

Department of Organic Chemistry "U. Schiff", University of Firenze, Via della Lastruccia 13, I-50019 Sesto Fiorentino, Italy, Department of Clinical Physiopathology, Endocrinology Unit, University of Firenze, Viale G. Pieraccini 6, I-50134 Firenze, Italy, Serono International S.P.R.I., 12, Chemin des Aulx, CH-1228 Plan-les Ouates, Geneve, Switzerland, and Department of Pharmaceutical Sciences, University of Bologna, Via Belmeloro 6, I-40126 Bologna, Italy

Received December 8, 2003

New 5α-reductase 1 (5αR-1) inhibitors were designed to complete a consistent set of analogues suitable for a 3D QSAR study. These compounds were synthesized by a modification of the aza-Robinson annulation, further functionalized by Pd-catalyzed cross-coupling processes, and were tested with human 5αR-1 expressed in Chinese hamster ovary 1827 cells. It turned out that the potency of the resulting inhibitors was strongly dependent on the type of substitution at the 8 position, with the IC_{50} values ranging from 8.1 to 1050 nM. The construction of this homogeneous set of molecules allowed a 3D QSAR study. In particular, comparative molecular field analysis (CoMFA) was used to correlate the potency of the inhibitors with their physicochemical features. Highly accurate evaluations of the atomic point charges were carried out by means of quantum chemical calculations at the DFT/B3LYP level of theory followed by the RESP fitting procedure. It turned out that increasing the reliability of electrostatic parameters greatly affected the statistical results of the QSAR analysis. The 3D QSAR model proposed could be very useful in the further development of 5αR-1 inhibitors, which are suitable candidates to be evaluated as drugs in the treatment of 5αR-1 related diseases such as acne and alopecia in men and hirsutism in women.

Introduction

The control of the biological action of steroids through the inhibition of specific enzymes involved in their metabolism, without significant changes in the overall profile of the other hormones, has represented an attractive pharmaceutical target during the past 20 years. For example, several androgen-dependent disorders and diseases such as prostate cancer, benign prostatic hyperplasia (BPH), acne and androgenetic alopecia in men, and hirsutism (associated with polycystic ovarian syndrome) in women appear to be related to 5α-dihydrotestosterone (DHT) production.[1−6] For this reason, much interest has been paid to the synthesis of inhibitors of 5α-reductase (5αR),[7,8] an enzyme that catalyzes the reduction of testosterone (T) to DHT.[9−10]

Steroid 5α-reductase (EC 1.3.99.5) is a membrane-bound, NADPH-dependent enzyme that catalyzes the selective, irreversible reduction of 4-ene-3-oxosteroids to the corresponding 5α-3-oxosteroids.[9,10] Two human isozymes of 5α-reductase have been cloned, expressed, and characterized (5αR-1 and 5αR-2), which have different chromosomal localization, tissue expression patterns, and enzyme kinetic parameters. Whereas the type 2 isozyme is found predominantly in the prostate, genital skin, seminal vesicles, epididymis, hair follicle, and liver, the type 1 isozyme occurs predominantly in sebaceous glands of the skin (including the scalp) and liver.[7−8,11] The pathologies associated with abnormal production of DHT and the relative importance of the two isoenzymes have been identified. In particular, the presence of the 5αR-1 isozyme in the scalp and skin has prompted an active research effort toward highly selective 5αR-1 inhibitors[12−17] for their use as therapeutic tools for the treatment of the pathologies of endocrine disorders such as androgenetic alopecia, male pattern baldness, acne in men, and hirsutism in women. The use of selective inhibitors of the 5αR-1 isoenzyme is mandatory for the treatment of women because it has been already ascertained that the inhibition of 5αR-2 can cause abnormalities in the male fetus.[18,19]

We have recently reported on a novel class of nonsteroidal inhibitors based on the benzo[*c*]quinolizin-3-ones structure (Figure 1).[17] The design of these compounds came from the observation that an increase of structural planarity in the corresponding 19-nor-10-azasteroidal 5α-reductase inhibitors[20,21] (obtained by introducing a double bond in the C ring, Figure 1)

* To whom correspondence should be addressed. For A.G.: phone and fax, +39 055 4573481/531; e-mail: antonio.guarna@unifi.it. For A.C.: phone and fax, +39 051 2099735/4; e-mail, andrea.cavalli@unibo.it.
[†] Department of Organic Chemistry "U. Schiff", University of Firenze.
[‡] Department of Clinical Physiopathology, University of Firenze.
[§] Serono International S.P.R.I.
[#] University of Bologna.

10.1021/jm031131o CCC: $27.50
Published on Web 06/08/2004

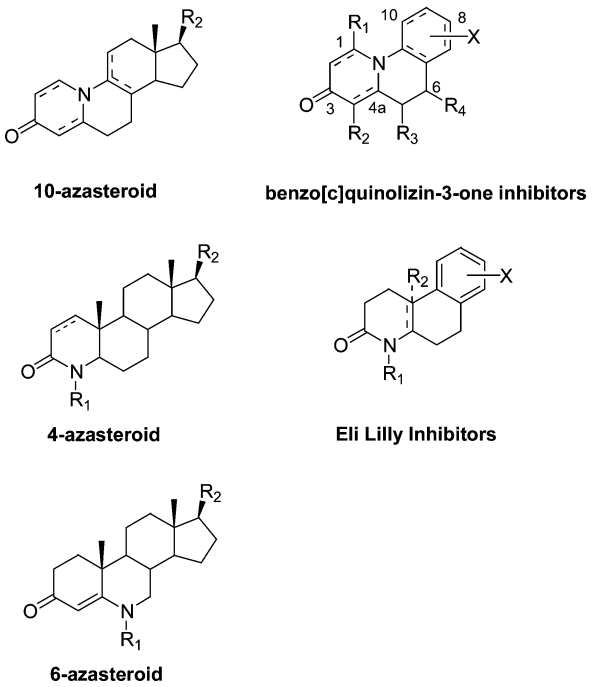

Figure 1. Structure of benzo[*c*]quinolizin-3-one and Eli Lilly inhibitors, with their azasteroid relative compounds.

Chart 1

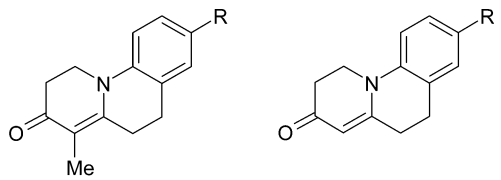

45 R=H
46 R=Cl
47 R=Me

48 R=H
49 R=Cl
50 R=Me

afforded molecules with higher inhibition potency toward 5αR-1 (Schemes 1−6 and Chart 1). Benzo[*c*]-quinolizin-3-ones, while maintaining the A ring enaminone moiety as an essential feature of the 19-nor-10-azasteroids, lacked the D ring and incorporated a benzene ring in place of the C ring to have a more planar overall structure. By analogy to the series of Eli Lilly compounds[13−16] (Figure 1), formally derived from 4-azasteroids, we found that benzo[*c*]quinolizin-3-one derivatives are selective and that some of them are very potent, competitive inhibitors of 5αR-1. The potency of these compounds depended on the presence and position of double bonds on the A ring and on the type and number of substituents introduced at positions 1, 4, 5, 6, and 8. Although only a limited series of compounds with variation of the group at position 8 were synthesized, we observed that the activity was strongly affected by this substituent (for example, compounds with a lipophilic group such as a methyl or a chlorine atom at position 8 were very active against 5αR-1).[17] Therefore, we synthesized and tested against 5αR-1 a series of molecules (Schemes 1−6 and Table 1) obtained by varying the group at the 8 position to assess its influence on the inhibitory activity. In particular, we introduced lipophilic substituents, from small aliphatic chains to larger aromatic and heteroaromatic moieties; benzyl ether groups, with different degree and type of substitution on the phenyl ring; and alkyl and phenyl ester groups, with various substituents on the phenyl ring. Some of these substituents have already proved to strongly affect the potency of the benzo[*f*]quinolinone inhibitors;[13−16] other have never been introduced in nonsteroidal 5α-reductase inhibitors. The only substituent that we maintained on the benzo[*c*]quinolizinone skeleton of these new series was the 4-methyl group, since its presence seems always associated with an increase of activity, irrespective of the group at position 8.[17] The construction of this homogeneous set of molecules would, moreover, allow a 3D QSAR study that, due to the lack of models for the active site of 5αR-1, would be very helpful in interpreting the biological data and in providing insight for the design of new inhibitors.

In this paper, we present the synthesis and the biological evaluation of some new 5αR-1 inhibitors designed to complete a consistent set of analogues suitable for a 3D QSAR study. Then we describe the development of a CoMFA model that attempts to correlate the biological activities of this series of 5αR-1 inhibitors with their physicochemical features. The model was obtained by taking into account the magnitude of the dipole moment and the log *P* of the molecules along with the classical electrostatic and steric CoMFA fields. Moreover, to enhance the quality of the description of the electrostatic contribution, density functional theory based computations were carried out to evaluate both the atomic partial charges and the dipole moment values of each inhibitor. Finally, the CoMFA model was validated by predicting the biological activities of a set

Table 1. Observed and Calculated (Using Model No. 6 of Table 2) 5αR-1 Inhibitory Activities of the Training Set[a]

	IC_{50} (nM)	pIC_{50} (obsd)	pIC_{50} (calcd)	Δ	log *P*	|ρ|
12	8.10	8.09	7.95	0.14	3.88	2.44
13	178	6.74	6.70	0.04	2.87	5.69
14	111	6.95	6.85	0.10	4.64	5.60
15	194	6.71	6.44	0.27	5.35	6.73
16	93.0	7.03	7.01	0.02	5.35	5.54
17	92.9	7.03	7.15	−0.12	5.35	5.07
18	83.7	7.08	7.15	−0.07	5.52	5.20
19	149	6.83	6.97	−0.14	6.41	5.28
20	393	6.41	6.64	−0.23	6.41	4.61
21	8.75	8.06	7.91	0.15	5.49	4.09
22	14.2	7.85	7.50	0.35	5.54	4.26
23	170	6.77	7.08	−0.31	3.35	3.47
26	380	6.42	6.44	−0.02	5.54	4.25
34	128	6.89	7.02	−0.13	4.74	4.48
35	117	6.93	6.57	0.36	3.13	3.09
36	221	6.66	6.60	0.06	3.66	3.30
37	731	6.14	6.07	0.07	3.97	3.83
38	1000	6.00	6.06	−0.06	4.37	4.02
39	96.8	7.01	6.83	0.18	4.96	3.39
40	942	6.03	5.92	0.11	4.64	3.12
41	560	6.25	6.32	−0.07	6.47	3.35
42	121	6.92	7.08	−0.16	4.86	2.24
44	1050	5.98	5.85	0.13	4.05	3.75
45[b]	185	6.73	7.11	−0.38	2.85	4.59
46[b]	5.80	8.25	7.95	0.30	3.73	2.35
47[b]	20.0	7.70	7.12	0.58	3.35	5.06
48[b]	298	6.53	6.87	−0.34	2.33	5.06
49[b]	49.0	7.31	7.72	−0.41	3.22	2.83
50[b]	376	6.42	6.84	−0.42	2.83	5.54

[a] The magnitude of the dipole moment (|ρ|) and the log *P* values are reported as well. [b] Compounds previously synthesized by us.[17]

Scheme 1[a]

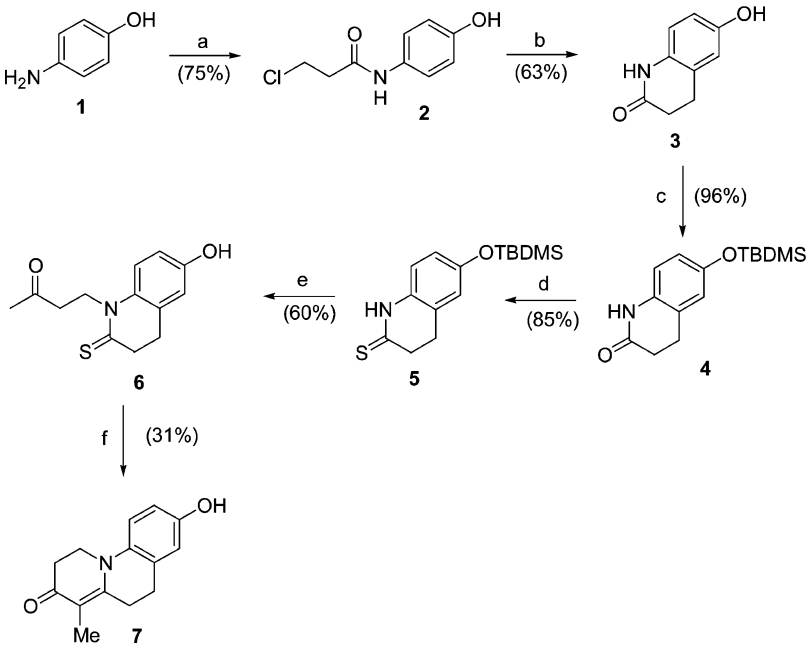

[a] (a) $ClCH_2CH_2COCl$, acetone, reflux, 1 h; (b) $AlCl_3$, fusion, 24 h; (c) TBDMSCl, Imidazole, DMF, 50° C, 2 h, then room temp, 14 h; (d) Lawesson's reagent, toluene, reflux, 15 min; (e) ethyl vinyl ketone, K_2CO_3, 18-crown-6, THF, room temp, 3 h; (f) Me_2SO_4, DBU, toluene, reflux, 40 min.

of molecules purposely synthesized and not used in deriving the 3D QSAR equations.

In this paper, besides proposing a model that rationalizes the QSAR of a series of 5αR-1 inhibitors, we present one of the first applications of density functional theory (DFT) in the building of a 3D QSAR model. Hopefully, this will help to strengthen the connection between theoretical physics and life sciences, which might provide enormous advantages in the drug design process as recently pointed out by a number of authors.[22]

Chemistry

All target inhibitors are 4-methylbenzo[*c*]quinolizin-3-ones bearing diverse substituents at the 8 position. We envisioned that the best strategy for the preparation of a large number of them was to have in hand a bulk quantity of a common intermediate to be easily, and possibly in a single step, transformed into the target compounds. Benzo[*c*]quinolizinones had been previously synthesized through a strategy based on a Mannich−Michael tandem reaction involving *N*-Boc iminium ions from lactams and 2-silyloxybutadiene derivatives,[17] but the methodology proved to be unsatisfactory in final yields and unsuitable for large-scale synthesis. More recently we have described a new synthetic route based on a modification of the aza-Robinson annulation still involving lactams as starting materials, which allowed us to prepare 4-methyl-substituted benzo[*c*]quinolin-3-ones in quantities up to 100 g.[23] For our purposes, we focused our attention on the synthesis of two derivatives to be used as common intermediates in the synthesis of most inhibitors, for instance, 8-hydroxy-4-methylbenzo-[*c*]quinolizin-3-one **7** (Scheme 1), whose 8-OH group could be functionalized in order to obtain ethers, and 8-bromo-4-methylbenzo[*c*]quinolizin-3-one **12** (Scheme 2), in which the aryl halide moiety could be used in Pd-

Scheme 2[a]

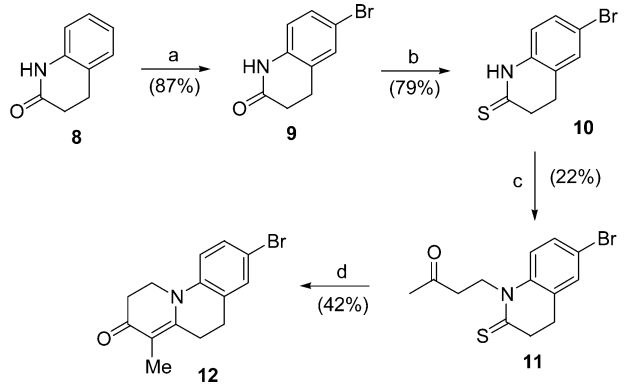

[a] (a) NBS, DMF, 0° C, 2 h; (b) Lawesson's reagent, toluene, reflux, 15 min; (c) ethyl vinyl ketone, K_2CO_3, 18-crown-6, THF, room temp, 3 h; (d) Me_2SO_4, DBU, toluene, reflux, 40 min.

catalyzed cross-coupling reactions for the preparation of 8-alkenyl- and alkynyl derivatives, and carbopalladation reactions for the introduction of ester moieties. Our modification of the aza-Robinson annulation proved to be suitable for the preparation of both compounds **7** and **12** as depicted in Schemes 1 and 2.

Regarding the synthesis of compound **7** (Scheme 1), 4-hydroxyaniline **1** was initially converted by treatment with *β*-chloropropionyl chloride to amide **2**, which underwent an intramolecular Friedel−Crafts alkylation by fusion at high temperature in the presence of $AlCl_3$ to give lactam **3** in 63% yield. After protection of the hydroxy group as a TBDMS ether, Lawesson's reagent was used to obtain thiolactam **5** (85% yield), which was subsequently N-alkylated with ethyl vinyl ketone in THF and in the presence of potassium carbonate as a base to give **6** in 60% yield, with the TBDMS protection being lost in the latter reaction. The final cyclization was achieved through generation of the thioiminium ion by treatment first with Me_2SO_4 in refluxing toluene and

Scheme 3[a]

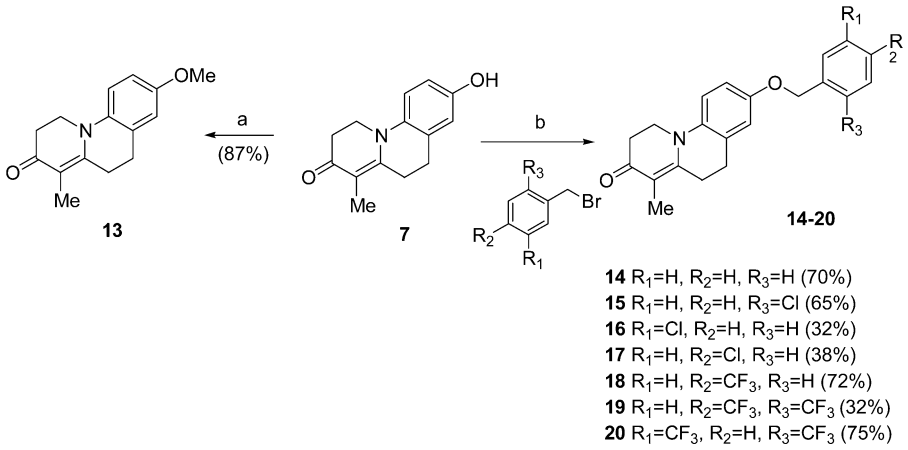

[a] (a) MeI, K_2CO_3, acetone, reflux, 8 h; (b) K_2CO_3, acetone, reflux, 6 h.

Scheme 4[a]

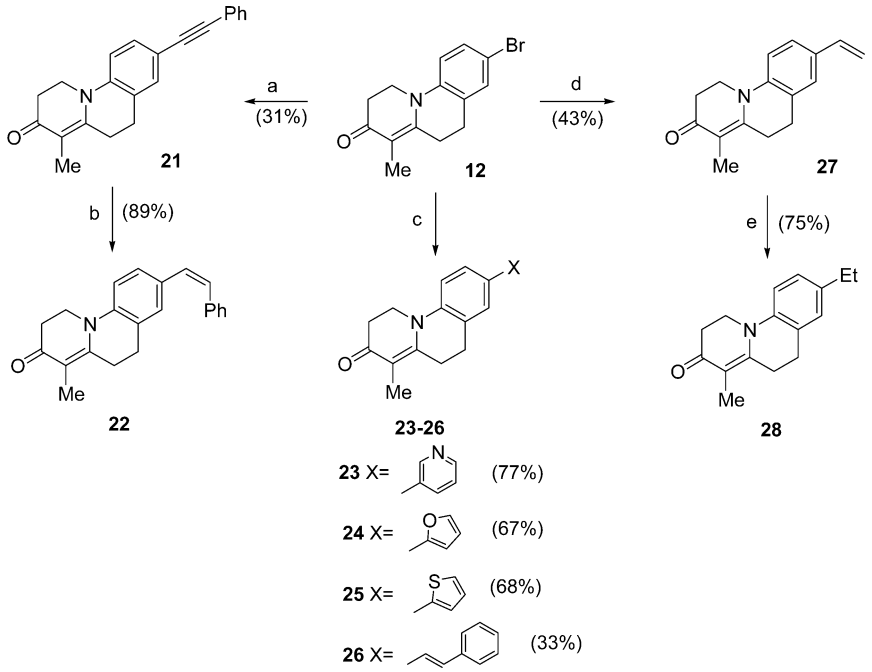

[a] (a) PhCCH, $PdCl_2(PPh_3)_2$, CuI, Et_3N, reflux, 6 h; (b) H_2, Pd/$BaSO_4$, pyridine, room temp, 16 h; (c) R_2BX, $PdCl_2(PPh_3)_2$, Na_2CO_3(aq) 2 M, THF, 80° C, 4−24 h; (d) $Bu_3SnCH{=}CH_2$, $Pd(OAc)_2$, PPh_3, Et_3N, 95° C, 24 h; (e) H_2, $(PPh_3)_3RhCl$, C_6H_6, 40° C, 6 h.

then with DBU as a base to give **7** in 31% yield after chromatography.

The synthesis of **12** was carried out (Scheme 2) starting from commercially available lactam **8**. This was easily converted to bromo derivative **9** by using *N*-bromosuccinimide in DMF. By application of the same strategy as above, after formation of the thiolactam **10**, in this case a low yield (22%) was obtained in the N-alkylation step to give **11**. This result was essentially due to competitive S-alkylation of the thiolactam. Despite this, after the final cyclization compound **12** was obtained in sufficient amount for all subsequent functionalizations.

As mentioned above, compound **7** was used as the starting material for the preparation of ethers (Scheme 3); 8-methoxyquinolizinone **13** was obtained in 87% yield by treatment with MeI in refluxing acetone and in the presence of K_2CO_3. Also, a wide variety of substituted benzyl ethers (**14**−**20**) were prepared with the same procedure using substituted benzyl bromides in yields ranging from 32% to 75% after chromatographic purification.

8-Bromo-4-methylbenzo[*c*]quinolizin-3-one **12** was a more versatile precursor for the introduction of new substituents on position 8 because of the possibility of performing a series of different Pd-catalyzed coupling reactions, including Sonogashira, Stille, Suzuki−Miyaura, and carbopalladation reactions. The first three processes were used for the introduction of small- to medium-sized lipophilic groups and heterocyclic rings on position 8. Under the conditions of the Sonogashira reactions, **12** reacted with phenylacetylene (Scheme 4) to give alkynyl derivative **21** in 31% yield. In this case, conversion to **21** was not complete, but we were lucky to witness precipitation of the coupling product in Et_3N (used as a base and solvent) mixed with triethylammonium salts. Derivative **21** was afterward hydrogenated to **22** over Lindlar catalyst to obtain the Z alkenyl derivative **22**

Scheme 5[a]

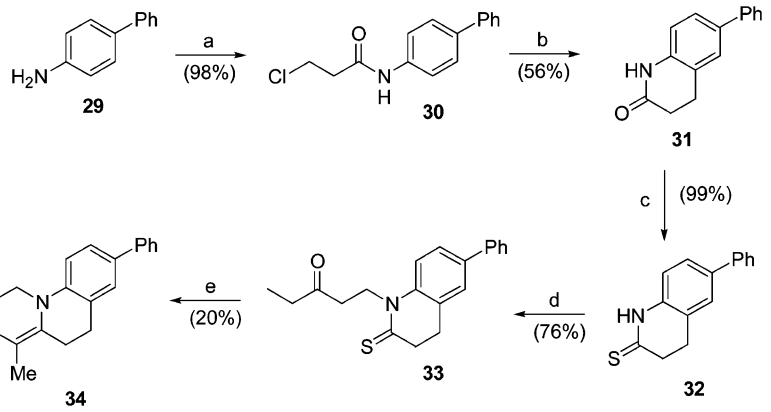

[a] (a) $ClCH_2CH_2COCl$, acetone, reflux, 1 h; (b) $AlCl_3$, fusion, 6 h; (c) Lawesson's reagent, toluene, reflux, 15 min; (d) ethyl vinyl ketone, K_2CO_3, 18-crown-6, THF, room temp, 3 h; (e) Me_2SO_4, DBU, toluene, reflux, 40 min.

Scheme 6[a]

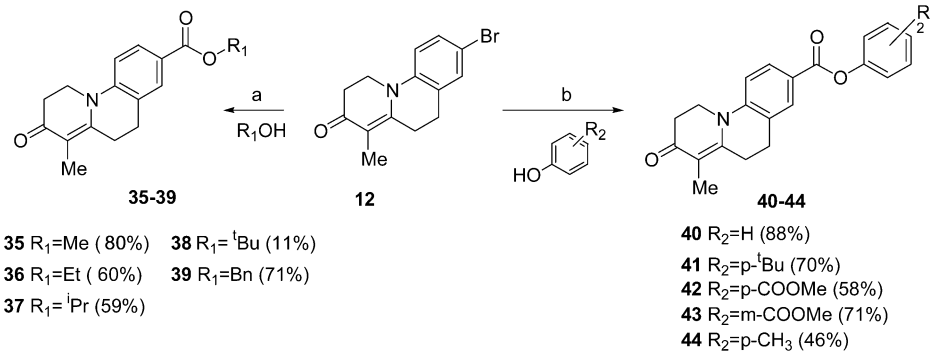

[a] (a) R_1OH, PPh_3CO, $PdCl_2$, Et_3N, C_6H_6, 115 °C, 24 h; (b) $R_2C_6H_4OH$, PPh_3CO, $PdCl_2$, Et_3N, C_6H_6, 115 °C, 24 h.

(89% yield after chromatography). These conditions ensured regioselectivity, since only partial reduction of the triple bond occurred. Suzuki−Miyaura cross-couplings were employed in order to insert heterocyclic substituents on the tricyclic structure (Scheme 4); 3-pyridyl, 2-furanyl, and 2-thiofenyl derivatives **23**, **24**, and **25**, respectively, were easily prepared performing couplings with the suitably substituted boronic acids at 80 °C under $(Ph_3P)_2PdCl_2$ (5%) catalysis in THF with 2 M Na_2CO_3(aq) as a base. The couplings were complete in 4−24 h and afforded products in 67−77% yield after chromatography. Synthesis of *E* styryl derivative **26** was achieved in a similar way; the Suzuki reaction was carried out under the same conditions as above with 2-styrylbenzo[1,3,2]dioxaborole prepared by addition of catecholborane to phenyl acetylene and gave **26** in 33% yield after chromatographic purification. A Stille cross-coupling was finally exploited to obtain vinyl derivative **27** (Scheme 4), employing tributylvinylstannane as the nucleophilic reagent. Selective hydrogenation of the vinyl moiety, leaving the enaminone moiety unaltered, was achieved by using the Wilkinson catalyst. This last reaction was carried out in benzene at 40 °C and was complete in 6 h, affording **28** in 75% yield.

The synthesis of 8-phenyl-substituted compound **34** (Scheme 5), which is structurally related to the heterocyclic derivatives **23**−**26**, could be realized through a Suzuki reaction using phenylboronic acid. However, we did not evaluate this possibility, since this compound had previously been obtained starting from commercially available biphenyl-4-ylamine **29** by employing the thiolactam-based strategy already described for **7** and **12**, as depicted in Scheme 5.

Benzo[*c*]quinolizin-3-ones, bearing ester groups on position 8, were obtained by carbopalladation of 8-Br derivative **12** in the presence of a nucleophile (alcohols and phenols were used) under high pressure (50 bar) of CO (Scheme 6). We employed the same reaction conditions in all cases, only increasing the amount of the catalyst in the case of poorer nucleophiles such as phenols bearing an electron-withdrawing group on the ring. The reactions were conducted in a steel autoclave, using 5% $PdCl_2$ as a catalyst in the presence of 10% Ph_3P with Et_3N as a base and in benzene as a solvent for 24 h at 120 °C. Different equivalents of nucleophile were used. Yields of carbopalladation ranged from 46% to 88% after chromatography, with the exception of the *tert*-butyl ester derivative **38**, which underwent acid-catalyzed hydrolysis during purification on silica gel, and the *p*-tolyl ester derivative **44**, which required an additional chromatographic purification. By this methodology, alkyl esters **35**−**39** with increasing bulkiness in the alcoholic moiety R_1 were prepared, as well as aryl esters **40**−**44** with polar and lipophilic substituents R_4 on the aromatic moiety.

Inhibition Tests

The synthesized compounds were tested with the human recombinant isozyme of 5αR-1 to evaluate the inhibitory potency using finasteride as a control.[17a,24] The assays were performed using stably transfected Chinese hamster ovary (CHO) 1827 cells[25] incubated for

Table 2. Summary of the PLS Runs with Different Sets of Independent Variables and Quantum Chemical Levels of Theory for the Electrostatics Calculations[a]

model no.	independent variables	optimal no. of components	q^2	s_{cross}	F	r^2	s	contribution			
								steric	electrostatic	log P	$\|\rho\|$
1	steric only	4	0.480	0.484	3.381	0.887	0.225	1.000			
2	electrostatic only	2	0.260	0.554	1.289	0.672	0.369		1.000		
3	steric and electrostatic	3	0.542	0.445	1.290	0.836	0.266	0.332	0.668		
4	steric, electrostatic, and log p	3	0.526	0.453	4.061	0.784	0.305	0.319	0.607	0.075	
5	steric, electrostatic, and dipole moment	4	0.591	0.429	5.290	0.892	0.220	0.233	0.625		0.143
6	**steric, electrostatic, log p, and dipole moment (DFT)[b]**	**3**	**0.628**	**0.401**	**6.197**	**0.841**	**0.262**	**0.233**	**0.548**	**0.060**	**0.159**
7	steric, electrostatic, log p, and dipole moment (PM3)[c]	3	0.229	0.577	1.087	0.628	0.401	0.479	0.384	0.037	0.099

[a] The analysis illustrated by the contour maps of Figure 2 is bold. [b] Both partial charges and dipole moment are calculated at the DFT level. [c] Both partial charges and dipole moment are calculated at the PM3 level.

30 min with ^{3}[H]-testosterone at the K_m concentration (2 μM for 5αR-1) and each inhibitor in the $10^{-9}-10^{-5}$ M concentration range. Data were processed with the program ALLFIT[26] using the four-parameter logistic equation to calculate the IC_{50} values. The interassay reproducibility of the method was good as assessed by calculating the mean IC_{50} of finasteride, which resulted in 911 ± 85 nM (CV = 9.4%, n = 15) and 21 ± 1.8 nM (CV = 8.6%, n = 12) for 5αR-1 and 5αR-2, respectively, consistent with the established selectivity reported for the inhibitor.[19]

For the mechanism of action of the control inhibitor finasteride toward human recombinant 5αR-1, it was demonstrated that finasteride behaves as an irreversible or psudoirreversible inhibitor when tested in the intact cell system.[19] Finastride was described as an active site directed slow time dependent inhibitor of human 5αR-1.[27]

Molecular Modeling

The molecular models were built by properly modifying the crystallographic 19-nor-10-aza-androstenedione skeleton retrieved from the Cambridge Structural Database.[21] After minimization, the inhibitors were thoroughly studied by means of Monte Carlo conformational searches, and the conformers were classified using cluster analysis.

The conformations chosen for the 3D QSAR analyses were further optimized at the DFT level, and the partial charges of the compounds were evaluated by means of the restrained electrostatic potential (RESP) fitting procedure.

The 3D QSAR analyses were carried out using the CoMFA method. The alignment of the molecules within the Cartesian space was accomplished by superimposing atom by atom the benzo[*c*]quinolizin-3-one skeleton of the set of compounds. The molecules bearing a flexible group at position 8 of the benzo[*c*]quinolizin-3-one moiety were aligned by using the *Z* and *E* styryl derivatives **22** and **26** as templates.

Results

The inhibitory potency of the present series of 5αR-1 inhibitors is reported in Table 1. The newly synthesized compounds (**12**−**44**) are all, with a few exceptions, good 5αR-1 inhibitors, with IC_{50} values ranging from 8 nM to roughly 1 μM.[23] To quantitatively rationalize the structure−activity relationships of the series of compounds, a 3D QSAR model was developed by employing the CoMFA procedure. To this aim, several statistical analyses (PLS) were carried out to establish the best set of independent variables to be used for the calculation of the CoMFA model. The DFT-calculated dipole moment and the log *P* values were taken into account along with the classical CoMFA independent variables (steric and electrostatic fields). In Table 2, the statistics of the PLS runs carried out with the steric and electrostatic fields only, those with the two fields plus either dipole moment or log *P* values, and finally, the PLS analysis with all of the computed independent variables are reported. Moreover, to assess the relevance of the DFT-based electrostatic calculations, CoMFA analyses with geometries, charges, and dipole moments calculated at the PM3 semiempirical level were also carried out (model no. 7, Table 2). Clearly, the computations at the DFT level greatly improved the statistics of the PLS analyses even though, concerning the geometry, the semiempirical PM3 and the ab initio DFT calculations provided fairly similar results (the mean rmsd of non-hydrogen atoms between PM3- and DFT-optimized molecules was equal to 0.26 Å).

Table 3. Observed and Calculated 5αR-1 Inhibitory Potency of the Test Set[a]

	IC_{50} (nM)	pIC_{50} (obsd)	pIC_{50} (calcd)	Δ	log P	$\|\rho\|$
24	133	6.88	7.30	−0.42	4.12	4.81
25	79	7.10	7.19	−0.09	4.62	4.35
27	21.6	7.67	7.52	0.15	3.57	4.15
28	14	7.85	7.12	0.73	3.88	5.03
43	965	6.02	6.14	−0.12	4.86	3.60

[a] The predictions were obtained by using model no. 6 of Table 2.

The best CoMFA analysis for the training set of 5αR-1 inhibitors (Table 1) was that obtained by taking into account both the dipole moment and log *P* values along with steric and electrostatic fields (model no. 6, Table 2). The use of these variables afforded the best statistics for both cross-validated and non-cross-validated PLS. The selected 3D QSAR model has an optimal number of components equal to 3 and descriptive and predictive abilities evaluated by the statistical parameters r^2 = 0.841 and s = 0.262, and q^2 = 0.628 and s_{cross} = 0.401. In addition, the predictive properties of the CoMFA model were more rigorously tested by calculating the 5αR-1 inhibitory potency of a set of molecules purposely synthesized and tested (Table 3). The resulting predictive correlation coefficient r^2_{pred} was equal to 0.676.[40]

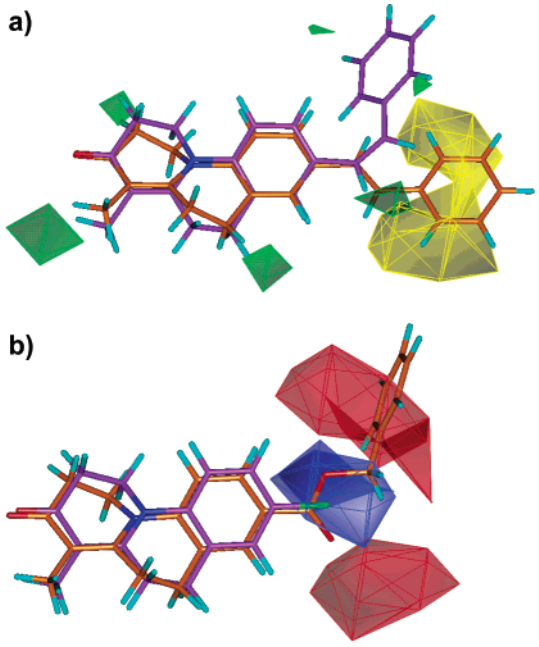

Figure 2. (a) View of the steric CoMFA STDEV*COEFF contour maps. The regions where increasing the molecular volume increases 5αR-1 inhibitory activity are green (0.0035 level), and the regions where increasing the volume decreases the activity are yellow (−0.012 level). The inhibitors shown are the *Z*-**22** (violet) and *E*-**26** (orange) diastereoisomers of the phenylvinyl derivative. (b) View of the electrostatic CoMFA STDEV*COEFF contour maps. The regions where increasing the positive charges increases 5αR-1 inhibitory activity are red (0.03 level), and the regions where increasing the negative charges increases the activity are blue (−0.02 level). The inhibitors shown are our most potent 5αR-1 inhibitors **46** (violet) and **39** (orange).

Thus, r^2_{pred} turned out to be of the same order of magnitude as q^2 and it can therefore be considered satisfactory.

The CoMFA model no. 6 accounting for the 3D QSAR of compounds of Table 1 is illustrated by the contour maps shown in Figure 2. Sterically favorable regions (Figure 2a, green contours) are quite split with a main appearance around the 4-methyl group, which was already pointed out as a fundamental substituent for an optimal 5αR-1 inhibitory profile.[17a] Sterically unfavorable regions (Figure 2a, yellow contours) are located around the substituent at position 8. In particular, the phenyl group of the styryl-substituted derivative **26** (diastereoisomer *E*, orange in Figure 2a), along with all inhibitors aligned onto it, protrudes inside the sterically unfavorable region, whereas the diastereoisomer Z (**22**, violet in Figure 2a) does not make any contact with that region. Electrostatic positive and negative regions (Figure 2b) are located around the substituent at position 8 as well. In particular, the negative CoMFA contours (blue) are close to the C8 atom of the benzo[*c*]quinolizinone moiety, where the chlorine (compound **46**, violet in Figure 2b) and the bromine (compound **12**) atoms, as well as the triple bond of **21**, and the oxygen atoms of **14**−**19**, **35**, **36**, **39** (orange in Figure 2b), and **42** are located. This means that in such a region, where relatively more potent compounds orient their 8-substituent, an increase of negative electrostatic potential should provide more potent 5αR-1 inhibitors. Concerning the positive electrostatic CoMFA contours (Figure 2b, red), two main regions were identified. One (bottom) was generated around both the carbonyl oxygen of the esters **35**, **36**, **39**, and **42**, as well as the sp^3 oxygen of the ethers and esters **20**, **37**, **38**, **40**, and **41**. The other (top) corresponded to the carbonyl oxygen of **37**, **38**, **40**, and **41**, as well as to the phenyl ring of the inhibitors aligned onto **22** (**14**−**19**, **35**, **36**, **39**, **42**), the latter being clearly embedded in the electrostatic positive region. All these molecules are of relatively lower potency than **12**, **21**, and **46**, and for this reason, the graphical model shows some apparently contradictory features. However, our interpretation is that an increase of the positive electrostatic potential in that region is required in order to obtain more potent compounds.

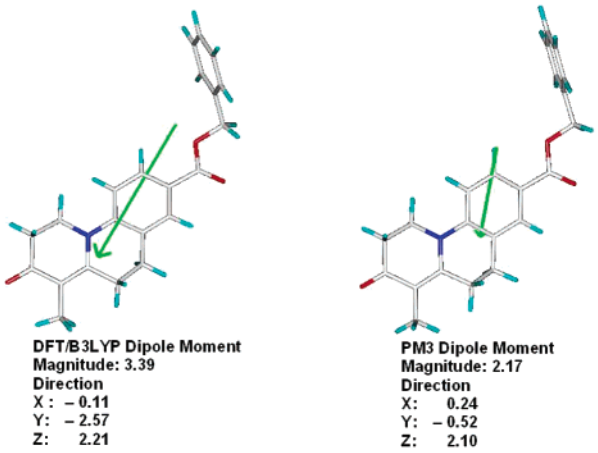

Figure 3. Dipole moment vector of compound **39** calculated at DFT/B3LYP (left) and PM3 semiempirical (right) levels. This physical observable is quite different between the two quantum chemical levels of theory in terms of both magnitude and direction.

The contributions to the CoMFA model of both the magnitude of the dipole moment ($|\rho|$) and log *P* are shown in Table 2. These values indicate a higher contribution of $|\rho|$ than log *P* to the calculated biological activity. Moreover, from the data of Table 1, it appears that a decrease of $|\rho|$ is associated with an increase of the inhibitory potency, whereas it seems that log *P* has to be increased to obtain more potent compounds.

Concerning the dipole moment, these were also estimated at the PM3 semiempirical level. In Figure 3, the dipole moment of compound **39**, calculated at DFT (left) and PM3 (right) levels, is reported. The dipole moment is shown in green, and the vector is reported in terms of magnitude and *X*, *Y*, and *Z* components. It clearly appears that the dipole moment was poorly estimated by PM3 with respect to that evaluated ab initio, in terms of both vector magnitude and direction (i.e., the orientation of the vector in Cartesian space).

Discussion

In this study, we present a CoMFA model for a series of 5αR-1 inhibitors currently under investigation for the treatment of several related endocrine disorders. Our CoMFA model describes the 3D QSAR for a series of benzo[*c*]quinolizin-3-one derivatives, of which a few have already been reported.[17] So far, interpretation of the inhibition experimental results has been based on

qualitative structure−activity relationships.[17] We have already shown that the overall planarity of the benzo[*c*]quinolizinones could be a fundamental feature for good binding with 5αR-1,[17a] although favorable interactions between the C-ring unsaturations and the enzyme active site should also be taken into account.[28] Besides this important feature, ring substitution plays a fundamental role in modulating the inhibitory activity. We have already shown, for example, that changing the position of a single methyl group on the benzo[*c*]quinolizin-3-one structure can dramatically affect the inhibition potency.[17] In particular, substitution at the 8 position had a major effect on the activity, and for this reason, we undertook this study aimed at obtaining, through a quantitative study, a deeper insight into these structure−activity relationships. To do this, an initial accurate evaluation of the atomic partial charges was carried out, and to our knowledge, for the first time a CoMFA model was developed using electrostatic computations at the DFT/B3LYP level. This was required because both the atomic partial charges and the dipole moment at the semiempirical quantum chemical level did not allow development of a significant 3D QSAR model (see Table 2). For the set of molecules under investigation in the present study, the electronic correlation effects seem to be of paramount importance to correctly describe the charge distribution. In fact, the high conjugation within the tricyclic system and the electron delocalization make the electronic correlation effects crucial for a correct description of the charge distribution as well as of chemical and geometrical features of the molecules. Therefore, an accurate treatment of the electrostatic properties of the molecules was required in order to achieve a good CoMFA model.

Model no. 6 of Table 2 shows that the electrostatic contribution to the final 3D QSAR equation is remarkably higher than the steric one. For example, in Figure 2a the steric CoMFA contour maps indicate that the positive steric contribution is almost irrelevant and mainly located around the 4-methyl group. This is in line with the fact that the most potent inhibitors of the series (**12** and **46**) do not bear a bulky substituent, indicating that their very high potency is more likely related to electrostatic effects. On the other hand, the negative steric contours (yellow) seem to be much more descriptive, accounting for the biological activities of the low potency inhibitors superimposed onto **26**.

Concerning the electrostatic CoMFA maps, they span very well-defined regions of the Cartesian space. This feature does not seem to be very often observed in CoMFA studies. In particular, the negative fragments at position 8 of the most and least potent inhibitors point inside the negative (blue in Figure 2b) and the positive (red in Figure 2b) electrostatic regions, respectively. Such an accurate description of the electrostatic 3D features of the series of 5αR-1 inhibitors was possible only for the 3D QSAR model built by using the DFT-based atomic partial charges. Thus, we can observe that ab initio quantum chemical calculations of geometry and electrostatics of the molecules can play a crucial role for the "standard" CoMFA procedures.

Moreover, the dipole moment and the log *P* values, included as independent variables in the computation of the 3D QSAR equation, indeed contributed to improve the statistics of the model (Table 2). Again, the dipole moment calculated at the semiempirical level was fairly different from those estimated by means of DFT (Figure 3), in terms of both magnitude and direction. This once more shows that the exchange and correlation electronic effects, which are well accounted for by means of DFT/B3LYP-based computations,[29] can be fundamental when evaluating physicochemical features for this series of molecules.

The importance of the dipole moment in both enzyme−inhibitor recognition and interaction has been recently pointed out by Sulpizi et al., who have performed a structure−activity relationship study on a series of inhibitors of herpes simplex virus type 1 thymidine kinase.[30] The dipole moment is a physicochemical parameter that accounts well for long-range interaction during the enzyme−inhibitor recognition phase, whereas the electrostatic field of the ligands may be useful to identify the interactions at the active site of the biological counterparts. In the present case, this might be taken to mean that our QSAR study not only reveals the role of physicochemical properties involved in the enzyme−inhibitor interaction (classical CoMFA fields) but also takes into account an aspect that can be related to the recognition phase between the ligands and their biological counterpart. However, Sulpizi et al. pointed out that the dipole moment could be important for the enzyme−inhibitor stabilization energy as well. Therefore, since so far we do not know anything about the three-dimensional features of the biological target (5αR-1), the present CoMFA model suggests a role for the dipole moment in driving both enzyme recognition and binding by the ligands. The determination of the 5αR-1 three-dimensional structure will hopefully verify such a hypothesis, allowing the study of these inhibitors in the light of the active site features of the enzyme.

Concerning log *P*, despite the low contribution of this parameter to the CoMFA model, it appears that an increase of the log *P* value might lead to more potent inhibitors. This is in good agreement with our previous observations that lipophilic groups at the 8 position increase the inhibitory potency,[17a] a feature also reported for some Eli Lilly compounds.[13−16] However, it should be noted that the experimental assays to assess the inhibitory potency are usually carried out in a cell system, which implies that the molecules have to pass the cell membrane to interact with the enzyme. Therefore, more hydrophobic inhibitors can penetrate through this barrier better than hydrophilic ones.

Conclusions

A 3D QSAR model was developed for a series of nonsteroidal 5αR-1 inhibitors having the benzo[*c*]quinolizin-3-one structure. These were synthesized by a modification of the aza-Robinson annulation and further functionalized by Pd-catalyzed cross-coupling processes and tested with human 5αR-1 expressed in CHO 1827 cells. The potency of the resulting inhibitors was strongly dependent on the type of substitution at the 8 position, with the IC_{50} values ranging from 8.1 to 1050 nM. To obtain a robust statistical model in building the 3D QSAR model, two "nonstandard" variables had to be added to the classical CoMFA fields, i.e., dipole moment

and log *P*. Moreover, the statistics of the 3D QSAR equation were greatly affected by the point charges and dipole moment accuracy. In particular, DFT calculations using the exchange and correlation functional B3LYP were required to get charges and dipole moment to be employed in the PLS analyses. In this respect, this paper represents one of the first examples in medicinal chemistry in which the QSAR was obtained by calculating parameters at the DFT quantum chemical level. We believe that the rapid increase in CPU speed will make such calculations routine in future computational medicinal chemistry investigations and provide advantages in the drug design process.[22] Finally, the 3D QSAR model proposed could be very useful in the further development of these inhibitors, which are compounds amenable to evaluation as drugs in the treatment of 5αR-1 related diseases such as acne and alopecia in men and hirsutism in women.

Experimental Section

1. Chemistry. All the reactions were performed under nitrogen unless otherwise stated. Chromatographic separations were performed under pressure on silica gel using flash column techniques. R_f values refer to TLC carried out on 25 mm silica gel plates (Merck F254), with the same eluant indicated for the column chromatography. IR spectra were recorded on a Perkin-Elmer 881 spectrophotometer in $CDCl_3$ solution. ^{1}H NMR (200 MHz) and ^{13}C NMR (50.33 MHz) spectra were recorded on a Varian XL 200 instrument in $CDCl_3$ solution. Mass spectra were carried out via EI at 70 eV on 5790A-5970A Hewlett-Packard and QMD 1000 Carlo Erba instruments. Microanalyses were carried out with a Perkin-Elmer 240C elemental analyzer.

6-Hydroxy-3,4-dihydroquinolin-2(1*H*)-one (3). To a refluxing solution of *p*-aminophenol **1** (10.4 g, 95.3 mmol) in acetone (25 mL) was slowly added a solution of 3-chloropropanoyl chloride (5 mL, 52.4 mmol) in acetone (10 mL). Then the solution was refluxed for 1 h and finally cooled to room temperature. The resulting suspension was transferred into a flask containing a solution of 6 N HCl in water (150 mL), and the solution was extracted with 3 × 150 mL of diethyl ether. The organic phase was washed with a saturated solution of $NaHCO_3$ and brine, then dried over Na_2SO_4 and evaporated under reduced pressure, affording amide **2** (7.81 g, 75%) as a brown solid: mp 85−87 °C; ^{1}H NMR ($CDCl_3$) δ 7.33 (AB system, 2H), 7.11 (s, 1H), 6.77 (AB system, 2H), 3.85 (t, J = 6.4 Hz, 2H), 2.75 (t, J = 6.4 Hz, 2H). A flask equipped with a mechanical stirrer and containing compound **2** (7.7 g, 38.5 mmol) was put in an oil bath heated at 160 °C, and after complete melting of **2**, $AlCl_3$ (18.0 g, 193 mmol) was added in small portions and the mixture was left under stirring at 160 °C for 24 h. After the mixture was cooled to room temperature and then to 0 °C, 10% HCl (100 mL) was added and the mixture was extracted with EtOAc. The organic phase was dried over Na_2SO_4, and after concentration lactam **3** (3.96 g, 63%) was obtained as a dark-red solid sufficiently pure for the next step: ^{1}H NMR (DMSO-d_6) δ 6.91−6.76 (m, 3H), 3.06 (t, J = 7.5 Hz, 2H), 2.70 (t, J = 7.5 Hz, 2H); MS *m*/*z* 163 (M^+, 19), 134 (15), 109 (19), 91 (100).

6-(*tert*-Butyldimethylsilanyloxy)-3,4-dihydroquinolin-2(1*H*)-one (4). To a solution of hydroxylactam **3** (300 mg, 1.8 mmol) in dry DMF (5 mL) under a N_2 atmosphere, imidazole (310 mg, 4.5 mmol) and TBDMSCl (329 mg, 2.2 mmol) were added. The solution was heated to 50 °C for 2 h, then cooled and maintained at room temperature overnight. After this period the solution was diluted with 5% $NaHCO_3$ (25 mL) and extracted with petroleum ether and CH_2Cl_2. The organic phase was dried and concentrated, and the crude brown solid was purified by chromatography (EtOAc/petroleum ether 1:2, R_f = 0.28) to give **4** (490 mg, 96%) as white crystals: mp 151−153 °C; ^{1}H NMR ($CDCl_3$) δ 7.72 (s, 1H), 6.63−6.53 (m, 3H), 2.87 (t, J = 7.8 Hz, 2H), 2.56 (t, J = 7.8 Hz, 2H), 0.94 (s, 9H), 0.15 (s, 6H); ^{13}C NMR ($CDCl_3$) δ 171.9 (s), 151.3 (s), 131.3 (s), 124.8 (s), 119.6 (d), 118.6 (d), 116.1 (d), 30.6 (t), 25.6 (t), 25.5 (q), −4.5 (s), −4.5 (q); MS (*m*/*z*) 277 (M^+, 73), 220 (100). Anal. ($C_{15}H_{23}NO_2Si$) C, H, N.

6-(*tert*-Butyldimethylsilanyloxy)-3,4-dihydroquinolin-2(1*H*)-thione (5). A mixture of **4** (390 mg, 1.4 mmol) and Lawesson's reagent (284 mg, 0.7 mmol) was suspended in anhydrous toluene (8 mL) and then refluxed under nitrogen atmosphere for 15 min. The solution was then cooled to room temperature and evaporated. The residue was purified by chromatography (EtOAc/petroleum ether 1:15, R_f = 0.30) to give **4** (350 mg, 85%) as a yellow solid: ^{1}H NMR ($CDCl_3$) δ 9.54 (s, 1H), 6.71−6.61 (m, 3H), 3.04 (t, J = 7.8 Hz, 2H), 2.78 (t, J = 7.8 Hz, 2H), 0.94 (s, 9H), 0.16 (s, 6H).

6-(*tert*-Butyldimethylsilanyloxy)-1-(3-oxopentyl)-3,4-dihydroquinolin-2(1*H*)-thione (6). Compound **5** (350 mg, 1.2 mmol), anhydrous K_2CO_3 (378 mg, 2.7 mmol) (kept at 140 °C for 12 h before use), and 18-crown-6 (41 mg, 0.15 mmol) were suspended in anhydrous THF (20 mL). After the mixture was cooled to 0 °C, the first portion of ethyl vinyl ketone (160 μL, 1.6 mmol) was added dropwise under stirring and nitrogen atmosphere. After the addition was complete, the solution was left at 0 °C for 5 min and then at room temperature for 1 h. The solution was cooled again to 0 °C, and a second portion of ethyl vinyl ketone (160 μL, 1.6 mmol) was added. The solution was left under stirring for 1.5 h at room temperature, the reaction being monitored by TLC. Then Na_2SO_4 was added, and the solution was filtered and concentrated, providing crude **6**, which was purified by chromatography (EtOAc/petroleum ether 1:2, R_f = 0.13) affording pure **6** (190 mg, 60%) as a yellow solid: mp 157−159 °C; ^{1}H NMR ($CDCl_3$) δ 6.98 (d, J = 8.8 Hz, 1H), 6.70−6.64 (m, 2H), 4.70 (t, J = 7.7 Hz, 2H), 3.10 (t, J = 7.7 Hz, 2H), 2.97 (t, J = 7.7 Hz, 2H), 2.70 (t, J = 7.7 Hz, 2H), 2.47 (q, J = 7.3 Hz, 2H), 1.05 (t, J = 7.7 Hz, 3H).

8-Hydroxy-4-methyl-2,3,5,6,-tetrahydro-(1*H*)-benzo[*c*]-quinolizin-3-one (7). Compound **6** (150 mg, 0.57 mmol) was suspended under a nitrogen atmosphere in anhydrous toluene (10 mL), and then freshly distilled Me_2SO_4 (150 μL, 1.5 mmol) was added dropwise at room temperature and under stirring. After the addition was complete, the flask was placed in an oil bath at 140−150 °C. After the mixture was refluxed for 15 min, DBU (230 μL, 1.5 mmol) was added dropwise and the resulting solution was refluxed for a further 20 min. Then it was cooled to room temperature, diluted with CH_2Cl_2, and washed with water. The organic layer was dried over Na_2SO_4 and evaporated, affording an orange solid that was washed with MeOH. After this treatment, pure compound **7** (41 mg, 31%) was obtained as a yellow solid: ^{1}H NMR (DMSO-d_6) δ 6.67−6.52 (m, 3H), 3.72 (t, J = 7.7 Hz, 2H), 2.61−2.42 (m, 6H), 1.64 (s, 3H); ^{13}C NMR (DMSO-d_6) δ 188.7 (s), 156.1 (s), 152.0 (s), 132.5 (s), 127.8 (s), 114.5 (d), 114.3 (d), 113.3 (d), 103.0 (s), 44.6 (t), 35.1 (t), 25.9 (t), 24.3 (t), 9.9 (q); MS (*m*/*z*) 203 (6), 160 (6), 84 (100), 66 (84). Anal. ($C_{14}H_{15}NO_2$) C, H, N.

6-Bromo-3,4-dihydroquinolin-2(1*H*)-one (9). To a solution of 3,4-dihydroquinolin-2(1*H*)-one **8** (10.19 g, 69.3 mmol) in DMF (220 mL) cooled at 0 °C, a solution of *N*-bromosuccinimide (13.1 g, 73.4 mmol) in DMF (220 mL) was added dropwise. The mixture was stirred at 0 °C for 2 h, then water (440 mL) was added and the solution was extracted with EtOAc/toluene 1:1 (400 mL + 2 × 200 mL). The organic phase was washed with water (2 × 200 mL), then dried over Na_2SO_4 and evaporated, affording a white solid, which was purified by crystallization (EtOH/H_2O 8:2), providing pure **9** (13.63 g, 87%) as white crystals: ^{1}H NMR ($CDCl_3$) δ 8.87 (s, 1H), 7.28 (s, 1H), 7.26 (d, J = 8.8 Hz, 1H), 6.68 (d, J = 8.8 Hz, 1H), 2.93 (t, J = 8.1 Hz, 2H), 2.60 (t, J = 8.1 Hz, 2H).

6-Bromo-3,4-dihydroquinolin-2(1*H*)-thione (10). 10 was prepared as reported for **5**. Starting from **9** (6.01 g, 26.6 mmol) and refluxing the reaction mixture for 45 min, pure **10** (5.07 g, 79%) was obtained as a yellow solid after chromatography (EtOAc/petroleum ether 1:5, R_f = 0.30): ^{1}H NMR ($CDCl_3$) δ 9.53 (s, 1H), 7.30 (m, 2H), 6.70 (d, J = 8.8 Hz, 1H), 3.07 (t, J = 8.0 Hz, 2H), 2.85 (t, J = 8.0 Hz, 2H).

6-Bromo-1-(3-oxopentyl)-3,4-dihydroquinolin-2(1*H*)-thione (11). 11 was prepared as reported for **6**. Starting from **10** (1.80 g, 7.43 mmol), pure **11** (528 mg, 22%) was obtained as a yellow solid after chromatography (EtOAc/petroleum ether 1:9, $R_f = 0.24$): ^{1}H NMR ($CDCl_3$) δ 7.37−7.29 (m, 2H), 6.97 (d, $J = 8$ Hz, 1H), 4.70 (t, $J = 8.4$ Hz, 2H), 3.12 (t, $J = 7.3$ Hz, 2H), 2.96 (t, $J = 7.7$ Hz, 2H), 2.73 (t, $J = 7.3$ Hz, 2H), 2.43 (q, $J = 7.3$ Hz, 2H), 1.05 (t, $J = 7.3$ Hz, 3H).

8-Bromo-4-methyl-2,3,5,6,-tetrahydro-(1*H*)-benzo[*c*]-quinolizin-3-one (12). 12 was prepared as reported for **7**. Starting from **11** (528 mg, 1.62 mmol), pure **12** (199 mg, 42%) was obtained as an orange solid after chromatography (EtOAc/petroleum ether 1:1, $R_f = 0.32$): ^{1}H NMR ($CDCl_3$) δ 7.32 (dd, $J_1 = 8.8$ Hz, $J_2 = 2.6$ Hz, 1H), 7.24 (s, 1H), 6.79 (d, $J = 8.4$ Hz, 1H), 3.87 (t, $J = 7.7$ Hz, 2H), 2.77−2.61 (m, 6H), 1.79 (s, 3H); ^{13}C NMR ($CDCl_3$) δ 190.7 (s), 155.3 (s), 139.7 (s), 130.4 (d), 128.8 (s), 125.9 (s), 114.4 (d), 114.0 (d), 106.6 (s), 45.1 (t), 35.4 (t), 26.1 (t), 24.7 8t), 10.1 (q); MS (*m*/*z*) 293 (72), 292 (M^+, 72), 291 (77), 262 (16), 248 (14), 235 (15), 212 (17), 154 (20), 149 (23), 128 (19), 89 (18), 84 (100), 77 (25). Anal. ($C_{14}H_{14}BrNO$) C, H, N.

8-Methoxy-4-methyl-2,3,5,6,-tetrahydro-(1*H*)-benzo[*c*]-quinolizin-3-one (13). To a solution of **12** (40 mg, 0.17 mmol) in acetone (3 mL) under a nitrogen atmosphere, K_2CO_3 (120 mg, 0.87 mmol) and MeI (110 μL, 1.7 mmol) were added. The mixture was refluxed for 8 h, then cooled to room temperature, filtered, and concentrated, affording **13** (37 mg, 87%) as a yellow oil: ^{1}H NMR ($CDCl_3$) δ 6.86 (d, $J = 8.4$ Hz, 1H), 6.76−6.69 (m, 2H), 3.87 (t, $J = 7.7$ Hz, 2H), 3.77 (s, 3H), 2.76−2.58 (m, 6H), 1.79 (s, 3H); ^{13}C NMR ($CDCl_3$) δ 190.3 (s), 156.4 (s), 154.6 (s), 134.3 (s), 128.2 (d), 113.8 (d), 113.7 (s), 112.0 (d), 105.0 (s), 55.6 (q), 45.2 (t), 35.4 (t), 26.4 (t), 25.1 (t), 10.1 (q); MS (*m*/*z*) 243 (M^+, 85), 212 (56). Anal. ($C_{15}H_{17}NO_2$) C, H, N.

8-Benzyloxy-4-methyl-2,3,5,6,-tetrahydro-(1*H*)-benzo-[*c*]quinolizin-3-one (14). To a solution of **12** (40 mg, 0.17 mmol) in acetone (3 mL) under a nitrogen atmosphere, K_2CO_3 (120 mg, 0.87 mmol) and benzyl bromide (42 μL, 0.35 mmol) were added. The mixture was refluxed for 6 h, then cooled to room temperature, filtered, and concentrated, affording pure **14** (39 mg, 70%): ^{1}H NMR ($CDCl_3$) δ 7.39−7.33 (m, 5H), 6.84−6.78 (m, 3H), 5.02 (s, 2H), 3.87 (t, $J = 7.7$ Hz, 2H), 2.72−2.58 (m, 6H), 1.79 (s, 3H); ^{13}C NMR ($CDCl_3$) δ 190.2 (s), 156.3 (s), 153.6 (s), 136.9 (s), 134.4 (s), 128.5 (d), 128.1 (s), 127.9 (d), 127.3 (d), 114.8 (d), 113.7 (d), 113.1 (d), 105.0 (s), 70.4 (t), 45.2 (t), 35.4 (t), 26.4 (t), 25.1 (t), 10.1 (q); MS (*m*/*z*) 319 (M^+, 19), 228 (100), 200 (20), 91 (37), 86 (17). Anal. ($C_{21}H_{21}NO_2$) C, H, N.

8-(2-Chlorobenzyloxy)-4-methyl-2,3,5,6,-tetrahydro-(1*H*)-benzo[*c*]quinolizin-3-one (15). 15 was prepared as reported for **14**, starting from **12** (25 mg, 0.11 mmol) and using 2-chlorobenzyl bromide (45 mg, 0.22 mmol). After chromatography (EtOAc/petroleum ether 3:2, $R_f = 0.29$) pure **15** (25 mg, 65%) was obtained as a pale-yellow solid: mp 105−109 °C; ^{1}H NMR ($CDCl_3$) δ 7.51 (m, 1H), 7.37 (m, 1H), 7.30−7.24 (m, 2H), 6.86−6.80 (m, 3H), 5.14 (s, 2H), 3.89 (t, $J = 7.4$ Hz, 2H), 2.73−2.60 (m, 6H), 1.81 (s, 3H); ^{13}C NMR ($CDCl_3$) δ 190.3 (s), 156.3 (s), 153.4 (s), 134.7 (s), 134.6 (s), 132.5 (s), 129.3 (d), 129.0 (d), 128.7 (d), 128.5 (s), 126.9 (d), 114.8 (d), 113.8 (d), 113.2 (d), 105.2 (s), 67.6 (t), 45.3 (t), 35.5 (t), 26.4 (t), 25.2 (t), 10.2 (q); MS (*m*/*z*) 353 (M^+, 12), 228 (100), 200 (28), 125 (25), 83 (39), 71 (42), 57 (78). Anal. ($C_{21}H_{20}ClNO_2$) C, H, N.

8-(3-Chlorobenzyloxy)-4-methyl-2,3,5,6,-tetrahydro-(1*H*)-benzo[*c*]quinolizin-3-one (16). 16 was prepared as reported for **14**, starting from **12** (25 mg, 0.11 mmol) and using 3-chlorobenzyl bromide (45 mg, 0.22 mmol). After chromatography (EtOAc/petroleum ether 3:2, $R_f = 0.25$) pure **15** (12 mg, 32%) was obtained as a pale-yellow solid: mp 119−123 °C; ^{1}H NMR ($CDCl_3$) δ 7.43 (s, 1H), 7.27 (m, 1H), 6.85−6.79 (m, 3H), 5.02 (s, 2H), 3.89 (t, $J = 7.4$ Hz, 2H), 2.74−2.61 (m, 6H), 1.82 (s, 3H); ^{13}C NMR ($CDCl_3$) δ 190.2 (s), 156.2 (s), 153.3 (s), 139.0 (s), 134.7 (s), 134.5 (s), 129.7 (d), 128.1 (s), 128.0 (d), 127.2 (d), 125.1 (d), 114.9 (d), 113.7 (d), 113.1 (d), 105.2 (s), 69.6 (t), 45.2 (t), 35.4 (t), 26.4 (t), 25.1 (t), 10.1 (q); MS (*m*/*z*) 353 (M^+, 23), 228 (100), 200 (53), 172 (15), 125 (20), 89 (14), 57 (22). Anal. ($C_{21}H_{20}ClNO_2$) C, H, N.

8-(4-Chlorobenzyloxy)-4-methyl-2,3,5,6,-tetrahydro-(1*H*)-benzo[*c*]quinolizin-3-one (17). 17 was prepared as reported for **14**, starting from **12** (25 mg, 0.11 mmol) and using 4-chlorobenzyl bromide (45 mg, 0.22 mmol). After chromatography (EtOAc/petroleum ether 3:2, $R_f = 0.25$) pure **15** (15 mg, 38%) was obtained as a pale-yellow solid: mp 145−149 °C; ^{1}H NMR ($CDCl_3$) δ 7.36 (ps, 4H), 6.85−6.79 (m, 3H), 5.01 (s, 2H), 3.89 (t, $J = 7.4$ Hz, 2H), 2.73−2.61 (m, 6H), 1.81 (s, 3H); ^{13}C NMR ($CDCl_3$) δ 190.2 (s), 156.3 (s), 153.4 (s), 143.2 (s), 134.6 (s), 133.7 (s), 128.7 (d), 128.6 (d), 128.3 (s), 114.9 (d), 113.7 (d), 113.1 (d), 105.2 (s), 69.7 (t), 45.3 (t), 35.4 (t), 26.4 (t), 25.2 (t), 10.2 (q); MS (*m*/*z*) 353 (M^+, 31), 230 (47), 228 (100), 200 (82), 172 (24), 127 (29), 125 (58), 89 (25), 57 (18). Anal. ($C_{21}H_{20}ClNO_2$) C, H, N.

8-(4-Trifluoromethylbenzyloxy)-4-methyl-2,3,5,6,-tetrahydro-(1*H*)-benzo[*c*]quinolizin-3-one (18). 18 was prepared as reported for **14**, starting from **12** (40 mg, 0.17 mmol) and using 4-trifluoromethylbenzyl bromide (55 μL, 0.35 mmol). After chromatography (EtOAc/petroleum ether 1:1, $R_f = 0.29$) pure **18** (47 mg, 72%) was obtained as a pale-yellow solid: mp 107−111 °C; ^{1}H NMR ($CDCl_3$) δ 7.67−7.48 (m, 4H), 6.90−6.78 (m, 3H), 5.10 (s, 2H), 3.88 (t, $J = 8.2$ Hz, 2H), 2.73−2.61 (m, 6H), 1.81 (s, 3H); ^{13}C NMR ($CDCl_3$) δ 190.2 (s), 156.2 (s), 153.2 (s), 141.0 (s), 134.8 (s), 128.3 (s), 127.2 (2d, 2C), 125.4 (s), 114.8 (d), 113.7 (d), 113.1 (d), 105.2 (s), 69.5 (t), 45.2 (t), 35.4 (t), 26.4 (t), 25.1 (t), 10.2 (q) (CF_3 nd); MS (*m*/*z*) 387 (M^+, 19), 228 (100), 159 (21), 149 (56). Anal. ($C_{22}H_{20}F_3NO_2$) C, H, N.

8-(2,4-Bis-trifluoromethylbenzyloxy)-4-methyl-2,3,5,6-tetrahydro-(1*H*)-benzo[*c*]quinolizin-3-one (19). 19 was prepared as reported for **14**, starting from **12** (25 mg, 0.11 mmol) and using 2,4-bis-trifluoromethylbenzyl bromide (40 μL, 0.22 mmol). After chromatography (EtOAc/petroleum ether 2:3, $R_f = 0.21$) pure **19** (16 mg, 32%) was obtained as a pale-yellow oil: ^{1}H NMR ($CDCl_3$) δ 7.96−7.82 (m, 3H), 6.94−6.80 (m, 3H), 5.30 (s, 2H), 3.91 (t, $J = 7.7$ Hz, 2H), 2.76−2.63 (m, 6H), 1.83 (s, 3H); ^{13}C NMR ($CDCl_3$) δ 190.3 (s), 156.2 (s), 152.7 (s), 135.1 (s), 128.9 (2d, 2C), 128.4 (s), 126.1 (d), 123.1 (s), 120.7 (s), 115.6 (s), 114.7 (d), 113.8 (d), 113.1 (d), 105.4 (s), 65.8 (t), 45.2 (t), 35.3 (t), 26.3 (t), 25.1 (t), 10.1 (q); MS (*m*/*z*) 455 (M^+, 8), 234 (17), 228 (100), 200 (33), 177 (19), 160 (15) (2 CF_3 nd). Anal. ($C_{23}H_{19}F_3NO_2$) C, H, N.

8-(2,5-Bis-trifluoromethylbenzyloxy)-4-methyl-2,3,5,6-tetrahydro-(1*H*)-benzo[*c*]quinolizin-3-one (20). 20 was prepared as reported for **14**, starting from **12** (40 mg, 0.17 mmol) and using 2,5-bis-trifluoromethylbenzyl bromide (65 μL, 0.34 mmol). After chromatography (EtOAc/petroleum ether 1:1, $R_f = 0.21$) pure **20** (60 mg, 75%) was obtained as a yellow solid: mp 149−154 °C; ^{1}H NMR ($CDCl_3$) δ 8.06 (s, 1H), 7.82 (d, $J = 7.7$ Hz, 1H), 7.68 (d, $J = 7.7$ Hz, 1H), 6.90−6.81 (m, 3H), 5.24 (s, 2H), 3.88 (t, $J = 7.7$ Hz, 2H), 2.75−2.60 (m, 6H), 1.80 (s, 3H); ^{13}C NMR ($CDCl_3$) δ 190.2 (s), 156.2 (s), 152.9 (s), 137.3 (s), 135.2 (s), 134.0 (s), 128.5 (2s, 2C), 126.6 (d), 125.5 (d), 125.0 (d), 115.0 (d), 113.9 (d), 113.3 (d), 105.4 (s), 66.1 (t), 45.3 (t), 35.5 (t), 26.4 (t), 25.2 (t), 10.2 (q) (2 CF_3 nd); MS (*m*/*z*) 455 (M^+, 12), 228 (100), 200 (19). Anal. ($C_{23}H_{19}F_3NO_2$) C, H, N.

8-(Phenylethynyl)-4-methyl-2,3,5,6,-tetrahydro-(1*H*)-benzo[*c*]quinolizin-3-one (21). Under a N_2 atmosphere **12** (101 mg, 0.35 mmol), $PdCl_2(PPh_3)_2$ (12 mg, 0.017 mmol), and CuI (7 mg, 0.034 mmol) were suspended in 2 mL of anhydrous NEt_3, and then phenylacetylene (45 μL, 0.41 mmol) was added. The mixture was heated to reflux for 6 h. After this period, the mixture was cooled to room temperature and the yellow solid precipitated was separated from the solution, dissolved in Et_2O (20 mL), and washed with 3 × 10 mL of H_2O. The organic layer was dried over Na_2SO_4 and evaporated under reduced pressure, obtaining a yellow residue. Chromatography (CH_2Cl_2/MeOH 40:1, $R_f = 0.25$) afforded **21** with 31% yield: ^{1}H NMR ($CDCl_3$) δ 7.52−7.30 (m, 7H), 6.90 (d, $J = 8.5$ Hz, 1H), 3.92 (t, $J = 8.3$ Hz, 2H), 2.78−2.62 (m, 6H), 1.81 (s, 3H); ^{13}C NMR ($CDCl_3$) δ 190.5 (s), 155.2 (s), 140.3 (s), 131.3 (d), 131.1 (d), 130.7 (d), 128.2 (d), 128.0 (d), 126.5 (s), 123.3 (s),

116.1 (s), 112.7 (d), 106.8 (s), 89.1 (s), 88.9 (s), 45.0 (t), 35.5 (t), 26.1 (t), 24.7 (t), 10.2 (q); MS *m/z* 313 (M^+, 100), 284 (14), 256 (15). Anal. ($C_{22}H_{19}NO$) C, H, N.

8-*Z*-Styryl-4-methyl-2,3,5,6,-tetrahydro-(1*H*)-benzo[*c*]-quinolizin-3-one (22). In a Schlenk container **21** (20 mg, 0.06 mmol) was dissolved in pyridine (1 mL), then Pd/$BaSO_4$ (Pd 10%, 25 mg) was added. The reaction vessel was filled with H_2, and the mixture was stirred at room temperature for 16 h. The mixture was then diluted with 15 mL of Et_2O and filtered over a Celite layer, and then the solution was washed with 2 × 10 mL of H_2O, dried over Na_2SO_4, and evaporated under reduced pressure. The crude product was chromatographed (EtOAc/petroleum ether 1:1, $R_f = 0.31$), yielding pure **22** (17 mg, 89%) as a yellow solid: ^{1}H NMR ($CDCl_3$) δ 7.50−6.95 (m, 7H), 6.76 (d, J = 8.6 Hz, 1H), 6.50 (AB, 1H), 3.87 (t, J = 7.6 Hz, 2H), 2.69−2.59 (m, 6H), 1.79 (s, 3H); ^{13}C NMR ($CDCl_3$) δ 190.5 (s), 155.6 (s), 139.9 (s), 137.4 (s), 131.1 (s), 128.6 (d), 127.7 (d), 127.4 (d), 127.3 (d), 126.9 (s), 126.3 (d), 126.1 (d), 125.5 (d), 113.0 (d), 106.4 (s), 45.2 (t), 35.6 (t), 26.4 (t), 25.0 (t), 10.2 (q); MS *m/z* 315 (M^+, 45), 286 (67), 258 (41). Anal. ($C_{22}H_{21}NO$) C, H, N.

8-Pirid-3-yl-4-methyl-2,3,5,6,-tetrahydro-(1*H*)-benzo[*c*]-quinolizin-3-one (23). Under a N_2 atmosphere **12** (57 mg, 0.20 mmol) was dissolved in THF (3 mL), and then $PdCl_2(PPh_3)_2$ (14 mg, 0.02 mmol), the boronic acid $(HO)_2$BPy (49 mg, 0.30 mmol), and Na_2CO_3(aq) 2 M (0.7 mL) were added. The mixture was vigorously stirred and heated to 80 °C for 4 h, then cooled to room temperature. H_2O (6 mL) was added, and the mixture was extracted with 3 × 10 mL of Et_2O. The organic layer was washed with H_2O, dried over Na_2SO_4, and evaporated under reduced pressure, affording the crude product, which was chromatographed (CH_2Cl_2/MeOH 10:1, $R_f = 0.31$) to give pure **23** (45 mg, 77%) as a yellow solid: ^{1}H NMR ($CDCl_3$) δ 8.80 (d, J = 1.9 Hz, 1H), 8.53 (d, J = 3.3 Hz, 1H), 7.83 (d, J = 8.0 Hz, 1H), 7.44 (dd, J_1 = 8.5 Hz, J_2 = 1.9 Hz, 1H), 7.34 (d, J = 2.6 Hz, 1H), 7.31 (d, J = 5.2 Hz, 1H), 7.03 (d, J = 8.4 Hz, 1H), 3.95 (t, J = 7.5 Hz, 2H), 2.86−2.63 (m, 6H), 1.82 (s, 3H); ^{13}C NMR ($CDCl_3$) δ 190.6 (s), 163.2 (s), 155.5 (s), 148.0 (d), 147.8 (d), 140.5 (s), 135.7 (s), 133.7 (d), 132.1 (s), 130.8 (s), 127.4 (d), 126.2 (d), 123.5 (d), 113.4 (d), 45.1 (t), 35.5 (t), 26.3 (t), 25.0 (t), 10.2 (q); MS *m/z* 290 (M^+, 100), 261 (25), 247 (21), 233 (28), 84 (92). Anal. ($C_{19}H_{18}N_2O$) C, H, N.

8-Furan-2-yl-4-methyl-2,3,5,6,-tetrahydro-(1*H*)-benzo-[*c*]quinolizin-3-one (24). 24 was prepared as reported for **23**, starting from **12** (88 mg, 0.30 mmol) and using $(HO)_2$BFur (50 mg, 0.45 mmol). After chromatography (EtOAc/petroleum ether 1:1, $R_f = 0.42$) pure **24** (57 mg, 67%) was obtained as a yellow solid: ^{1}H NMR ($CDCl_3$) δ 7.52 (dd, J_1 = 8.8 Hz, J_2 = 1.8 Hz, 1H), 7.43 (ps, 2H), 6.94 (d, J = 8.8 Hz, 1H), 6.54 (d, J = 3.3 Hz, 1H), 6.44 (dd, J_1 = 1.8 Hz, J_2 = 1.5 Hz, 1H), 3.93 (t, J = 7.5 Hz, 2H), 2.82−2.62 (m, 6H), 1.82 (s, 3H); ^{13}C NMR ($CDCl_3$) δ 190.5 (s), 155.5 (s), 153.5 (s), 141.6 (d), 139.5 (s), 126.8 (s), 124.6 (s), 123.1 (2C, 2d), 113.0 (d), 111.6 (d), 106.3 (s), 103.9 (d), 45.1 (t), 35.5 (t), 26.3 (t), 24.9 (t), 10.2 (q); MS *m/z* 279 (M^+, 100), 250 (39), 222 (55), 140 (29), 83 (31). Anal. ($C_{18}H_{17}NO_2$) C, H, N.

8-Thiophen-2-yl-4-methyl-2,3,5,6,-tetrahydro-(1*H*)-benzo[*c*]quinolizin-3-one (25). 25 was prepared as reported for **23**, starting from **12** (88 mg, 0.30 mmol) and using $(HO)_2$BTfn (58 mg, 0.45 mmol). After chromatography (EtOAc/petroleum ether 3:2, $R_f = 0.45$) pure **24** (61 mg, 68%) was obtained as a yellow solid: ^{1}H NMR ($CDCl_3$) δ 7.46 (dd, J_1 = 8.5 Hz, J_2 = 2.2 Hz, 1H), 7.44 (d, J = 2.2 Hz, 1H), 7.21 (ps, 2H), 7.05 (dd, J_1 = 4.4 Hz, J_2=4.4 Hz, 1H), 6.93 (d, J = 8.5 Hz, 1H), 3.93 (t, J = 7.7 Hz, 2H), 2.82−2.62 (m, 6H), 1.82 (s, 3H); ^{13}C NMR ($CDCl_3$) δ 190.4 (s), 155.3 (s), 143.5 (s), 139.6 (s), 127.9 (s), 127.8 (d), 126.9 (s), 125.0 (d), 124.9 (d), 123.9 (d), 122.1 (d), 112.9 (d), 106.2 (s), 44.8 (t), 35.3 (t), 26.0 (t), 24.7 (t), 9.9 (q); MS *m/z* 295 (M^+, 100), 266 (23), 252 (19), 238 (24), 149 (25), 57 (37). Anal. ($C_{18}H_{17}NOS$) C, H, N.

8-*E*-Styryl-4-methyl-2,3,5,6,-tetrahydro-(1*H*)-benzo[*c*]-quinolizin-3-one (26). Under a N_2 atmosphere **12** (60 mg, 0.20 mmol) was dissolved in THF (3 mL), and then $PdCl_2(PPh_3)_2$ (14 mg, 0.02 mmol), the boronic ester (0.45 mmol), and Na_2CO_3(aq) 2 M (0.7 mL) were added. The mixture was vigorously stirred and heated to reflux for 24 h, then cooled to room temperature. H_2O (10 mL) was added, and the mixture was extracted with 3 × 10 mL of CH_2Cl_2. The organic layer was washed with H_2O, dried over Na_2SO_4, and evaporated under reduced pressure, affording the crude product, which was chromatographed using EtOAc/light petroleum 1:1 as eluant ($R_f = 0.27$). The pure product was obtained with 33% yield: mp 180−182 °C; ^{1}H NMR ($CDCl_3$) δ 7.50−7.23 (m, 7H), 7.02 (s, 2H), 6.92 (d, J = 8.4 Hz, 1H), 3.93 (t, J = 7.6 Hz, 2H), 2.82−2.62 (m, 6H), 1.82 (s, 3H); ^{13}C NMR ($CDCl_3$) δ 190.5 (s), 155.6 (s), 139.8 (s), 137.3 (s), 131.0 (s), 128.6 (d), 127.6 (d), 127.3 (d), 127.2 (d), 126.8 (s), 126.2 (d), 126.1 (d), 125.4 (d), 113.0 (d), 106.5 (s), 45.1 (t), 35.5 (t), 26.3 (t), 25.0 (t), 10.2 (q); MS *m/z* 315 (M^+, 100), 286 (36), 258 (38). Anal. ($C_{22}H_{21}NO$) C, H, N.

8-Vinyl-4-methyl-2,3,5,6,-tetrahydro-(1*H*)-benzo[*c*]quinolizin-3-one (27). Under a N_2 atmosphere **12** (100 mg, 0.34 mmol), $Pd(OAc)_2$ (4 mg, 0.017 mmol), and PPh_3 (18 mg, 0.068 mmol) were dissolved in anhydrous NEt_3, then tributylvinylstannane (150 mL, 0.51 mmol) was added. The solution was heated to 95 °C for 24 h. After this period, the solvent was evaporated, the residue was dissolved in 3 mL of EtOAc, 5 mL of KF(aq) 1 M were added, and the mixture was vigorously stirred for 1 h. The biphasic mixture was then filtered over Celite, and the filtrating agent was washed with EtOAc. The organic layer (25 mL) was separated from the aqueous layer, washed with brine (2 × 15 mL), dried over Na_2SO_4, and evaporated under reduced pressure, affording the crude product, which was chromatographed using EtOAc/light petroleum 1:1 as eluant ($R_f = 0.27$). The pure product was obtained with 43% yield. ^{1}H NMR ($CDCl_3$) δ 7.24 (d, J = 8.5 Hz, 1H), 7.19 (s, 1H), 6.88 (d, J = 8.5 Hz, 1H), 6.63 (dd, J_1 =17.6 Hz, J_2 =10.8 Hz, 1H), 5.64 (d, J = 17.6 Hz, 1H), 5.15 (d, J = 10.8 Hz, 1H), 3.91 (t, J = 7.7 Hz, 2H), 2.78−2.60 (m, 6H), 1.81 (s, 3H); ^{13}C NMR ($CDCl_3$) δ 190.5 (s), 155.7 (s), 139.9 (s), 135.8 (d), 131.2 (s), 126.6 (s), 125.7 (d), 125.2 (d), 112.8 (t), 112.3 (d), 106.2 (s), 45.1 (t), 35.5 (t), 26.3 (t), 24.9 (t), 10.2 (q); MS *m/z* 239 (M^+, 62), 238 (100), 210 (21), 182 (24). Anal. ($C_{16}H_{17}NO$) C, H, N.

8-Ethyl-4-methyl-2,3,5,6,-tetrahydro-(1*H*)-benzo[*c*]quinolizin-3-one (28). Into an autoclave 8-vinyl-Q1-4M (15 mg, 0.063 mmol) was dissolved in C_6H_6 (1 mL), and then the catalyst $(PPh_3)_3$RhCl (3 mg, 3.1 μmol) was added. The autoclave was filled with H_2 (100 psi) and was heated to 40 °C for 6 h. After this period the solvent was evaporated and the residue was dissolved in 10 mL of Et_2O and washed with H_2O (2 × 10 mL), then dried over Na_2SO_4 and evaporated under reduced pressure, affording the crude product, which was chromatographed using EtOAc/light petroleum ether 2:1 as eluant ($R_f = 0.33$). The pure product was obtained with 75% yield: ^{1}H NMR ($CDCl_3$) δ 7.04 (dd, J_1 = 8.5 Hz, 1H), 6.96 (s, 1H), 6.86 (d, J = 8.5 Hz,1H), 3.89 (t, J = 7.7 Hz, 2H), 2.78−2.52 (m, 8H), 1.80 (s, 3H), 1.20 (t, J = 8 Hz, 3H); ^{13}C NMR ($CDCl_3$) δ 190.4 (s), 156.3 (s), 138.0 (s), 137.4 (s), 127.2 (d), 126.7 (d), 126.5 (s), 112.7 (d), 105.5 (s), 45.1 (t), 35.5 (t), 28.0 (t), 26.4 (t), 24.9 (t), 15.7 (q), 10.1 (q); MS *m/z* 241 (M^+, 74), 226 (64), 198 (35), 83 (29). Anal. ($C_{16}H_{19}NO$) C, H, N.

6-Phenyl-3,4-dihydroquinolin-2(1*H*)-one (31). 31 was prepared as reported for **3**. Starting from **29** (5.00 g, 29.5 mmol), amide **30** was obtained in 98% yield: mp 177−179 °C; ^{1}H NMR ($CDCl_3$) δ 7.55 (ps, 5H), 7.52 (s, 1H), 7.43−7.30 (m, 4H), 3.88 (t, J = 6.6 Hz, 2H), 2.81 (t, J = 6.6 Hz, 2H); MS *m/z* 259 (M^+, 15), 169 (100). The cyclization of **30** (2.00 g, 7.7 mmol) to the corresponding lactam was carried out by heating at 180−190 °C for 6 h, obtaining **31** (961 mg, 56%) after purification by chromatography (EtOAc/petroleum ether 3:7, $R_f = 0.29$): ^{1}H NMR ($CDCl_3$) δ 7.77 (s, 1H), 7.53−7.20 (m, 7H), 6.80 (d, J = 8.5 Hz, 1H), 3.01 (t, J = 7.6 Hz, 2H), 2.65 (t, J = 7.6 Hz, 2H).

6-Phenyl-3,4-dihydroquinolin-2(1*H*)-thione (32). 32 was prepared as reported for **5**. Starting from **31** (230 mg, 1.03 mmol), **32** (243 mg) was obtained in 99% yield as an orange solid after purification by chromatography (CH_2Cl_2/petroleum

ether 4:3, $R_f = 0.26$): ^{1}H NMR ($CDCl_3$) δ 9.40 (s, 1H), 7.53−7.31 (m, 7H), 6.86 (d, $J = 8.5$ Hz, 1H), 3.12 (t, $J = 6.6$ Hz, 2H), 2.92 (t, $J = 6.6$ Hz, 2H).

6-Phenyl-1-(3-oxopentyl)-3,4-dihydroquinolin-2(1*H*)-thione (33). 33 was prepared as reported for **6**. Starting from **32** (243 mg, 1.02 mmol), pure **33** (250 mg, 76%) was obtained as a yellow solid after chromatography (EtOAc/petroleum ether 1:8, $R_f = 0.23$): ^{1}H NMR ($CDCl_3$) δ 7.56−7.29 (m, 7H), 7.17 (d, $J = 8.4$ Hz, 1H), 4.78 (t, $J = 9.1$ Hz, 2H), 3.18 (t, $J = 7.7$ Hz, 2H), 3.02 (t, $J = 7.7$ Hz, 2H), 2.83 (t, $J = 7.7$ Hz, 2H), 2.49 (q, $J = 7.3$ Hz, 2H), 1.07 (t, $J = 7.3$ Hz, 3H).

8-Phenyl-4-methyl-2,3,5,6,-tetrahydro-(1*H*)-benzo[*c*]-quinolizin-3-one (34). 34 was prepared as reported for **7**. Starting from **33** (250 mg, 0.77 mmol), pure **34** (45 mg, 20%) was obtained as a pale-yellow solid after chromatography (EtOAc/petroleum ether 45:70, $R_f = 0.28$): mp 161−165 °C; ^{1}H NMR ($CDCl_3$) δ 7.56−7.29 (m, 7H), 7.00 (d, $J = 8.8$ Hz, 1H), 3.94 (t, $J = 8.1$ Hz, 2H), 2.90−2.62 (m, 6H), 1.81 (s, 3H); ^{13}C NMR ($CDCl_3$) δ 190.5 (s), 166.7 (s), 155.9 (s), 140.3 (s), 135.3 (s), 132.7 (s), 128.8 (d), 127.0 (d), 126.6 (d), 126.4 (d), 126.2 (d), 113.2 (d), 106.2 (s), 45.1 (t), 35.5 (t), 26.3 (t), 25.0 (t), 10.1 (q); MS *m*/*z* 289 (M^+, 100), 260 (47), 246 (36), 232 (51) 165 (29), 57 (30). Anal. ($C_{20}H_{19}NO$) C, H, N.

8-Carboxymethyl-4-methyl-2,3,5,6,-tetrahydro-(1*H*)-benzo[*c*]quinolizin-3-one (35). Into an autoclave **12** (50 mg, 0.17 mmol), $PdCl_2$ (4 mg, 0.023 mmol), PPh_3 (12 mg, 0.046 mmol), NEt_3 (30 μL, 0.22 mmol), and MeOH (1 mL, 25 mmol) were mixed with 3 mL of benzene. The autoclave was filled with CO (50 bar) and then heated to 115 °C for 24 h. After this period the mixture was cooled to room temperature and the solvent and the excess alcohol were evaporated under reduced pressure, giving a yellowish residue. Chromatography of the crude product (eluant EtOAc/light petroleum 1:1, $R_f = 0.36$) afforded pure **35** (37 mg) with 80% yield: mp 106−108 °C; ^{1}H NMR ($CDCl_3$) δ 7.90 (dd, $J_1 = 8.8$ Hz, $J_2 = 2.0$ Hz, 1H), 7.78 (d, $J = 2.0$ Hz, 1H), 6.95 (d, $J = 8.8$ Hz, 1H), 3.95 (t, $J = 7.4$ Hz, 2H), 3.87 (s, 3H), 2.85−2.63 (m, 6H), 1.81 (s, 3H); ^{13}C NMR ($CDCl_3$) δ 190.6 (s), 166.5 (s), 154.6 (s), 144.1 (s), 130.3 (d), 128.9 (d), 122.9 (s), 112.2 (d), 107.7 (s), 51.9 (q), 45.1 (t), 35.5 (t), 26.0 (t), 24.8 (t), 10.2 (q); MS *m*/*z* 271 (M^+, 75), 242 (40), 227 (38), 214 (19). Anal. ($C_{16}H_{17}NO_3$) C, H, N.

8-Carboxyethyl-4-methyl-2,3,5,6,-tetrahydro-(1*H*)-benzo[*c*]quinolizin-3-one (36). 36 was prepared as reported for **35**, starting from **12** (50 mg, 0.17 mmol) and using EtOH (1 mL, 17 mmol). After chromatography (EtOAc/petroleum ether 1:1, $R_f = 0.34$) pure **36** (30 mg, 60%) was obtained as a white solid: mp 110−112 °C; ^{1}H NMR ($CDCl_3$) δ 7.90 (d, $J = 8.1$ Hz, 1H), 7.79 (s, 1H), 6.95 (d, $J = 8.1$ Hz, 1H), 4.34 (q, $J = 7.0$ Hz, 2H), 3.95 (t, $J = 7.3$ Hz, 2H), 2.79−2.63 (m, 6H), 1.81 (s, 3H), 1.37 (t, $J = 7.0$ Hz, 3H); ^{13}C NMR ($CDCl_3$) δ 190.7 (s), 166.1 (s), 154.7 (s), 144.0 (s), 129.6 (d), 128.9 (d), 126.1 (s), 123.2 (s), 112.2 (d), 107.6 (s), 60.7 (t), 45.1 (t), 35.5 (t), 26.0 (t), 24.7 (t), 14.4 (q), 10.2 (q); MS *m*/*z* 285 (M^+, 100), 256 (55), 240 (29), 77 (44). Anal. ($C_{17}H_{19}NO_3$) C, H, N.

8-Carboxyisopropyl-4-methyl-2,3,5,6,-tetrahydro-(1*H*)-benzo[*c*]quinolizin-3-one (37). was **37** prepared as reported for **36**, starting from **12** (50 mg, 0.17 mmol) and using 2-propanol (1 mL, 13 mmol). After chromatography (EtOAc/petroleum ether 1:1, $R_f = 0.37$) pure **15** (30 mg, 59%) was obtained as a white solid: mp 129−131 °C; ^{1}H NMR ($CDCl_3$) δ 7.90 (dd, $J_1 = 8.8$ Hz, $J_2 = 1.8$ Hz, 1H), 7.77 (d, $J = 1.8$ Hz, 1H), 6.94 (d, $J = 8.8$ Hz, 1H), 5.21 (hp, $J = 6.2$ Hz, 1H), 3.95 (t, $J = 7.7$ Hz, 2H), 2.85−2.63 (m, 6H), 1.81 (s, 3H), 1.34 (d, $J = 6.2$ Hz, 6H); ^{13}C NMR ($CDCl_3$) δ 190.7 (s), 165.5 (s), 154.7 (s), 143.9 (s), 129.6 (d), 128.8 (d), 126.0 (s), 123.7 (s), 112.1 (d), 107.6 (s), 68.0 (d), 45.1 (t), 35.5 (t), 26.0 (t), 24.8 (t), 22.0 (q), 10.2 (q); MS *m*/*z* 299 (M^+, 57), 256 (100), 240 (20). Anal. ($C_{18}H_{21}NO_3$) C, H, N.

8-Carboxy-*tert*-butyl-4-methyl-2,3,5,6,-tetrahydro-(1*H*)-benzo[*c*]quinolizin-3-one (38). 38 was prepared as reported for **36**, starting from **12** (50 mg, 0.17 mmol) and using *tert*-butyl alcohol (1 mL, 10 mmol). After chromatography (EtOAc/petroleum ether 1:1, $R_f = 0.29$) pure **38** (6 mg, 11%) was obtained as a white solid: mp 161−163 °C; ^{1}H NMR ($CDCl_3$) δ 7.84 (dd, $J_1 = 8.5$ Hz, $J_2 = 2.2$ Hz, 1H), 7.72 (s, 1H), 6.92 (d, $J = 8.5$ Hz, 1H), 3.94 (t, $J = 7.3$ Hz, 2H), 2.82−2.63 (m, 6H), 1.81 (s, 3H), 1.57 (s, 9H); ^{13}C NMR ($CDCl_3$) δ 193.5 (s), 168.5 (s), 155.8 (s), 142.4 (s), 129.5 (d), 128.8 (d), 126.0 (s), 123.0 (s), 112.1 (d), 107.5 (s), 63.5 (s), 45.1 (t), 35.5 (t), 28.3 (q), 26.1 (t), 24.8 (t), 10.2 (q); MS *m*/*z* 313 (M^+, 20), 256 (100), 240 (20), 83 (72). Anal. ($C_{19}H_{23}NO_3$) C, H, N.

8-Carboxybenzyl-4-methyl-2,3,5,6,-tetrahydro-(1*H*)-benzo[*c*]quinolizin-3-one (39). 39 was prepared as reported for **36**, starting from **12** (50 mg, 0.17 mmol) and using benzyl alcohol (1 mL, 10 mmol). After chromatography (EtOAc/petroleum ether 1:1, $R_f = 0.29$) pure **39** (42 mg, 71%) was obtained as a white solid: mp 107−110 °C; ^{1}H NMR ($CDCl_3$) δ 7.94 (dd, $J_1 = 8.8$ Hz, $J_2 = 2.2$ Hz, 1H), 7.81 (s, 1H), 7.44−7.34 (m, 5H), 6.94 (d, $J = 8.8$ Hz, 1H), 5.32 (s, 2H), 3.94 (t, $J = 7.4$ Hz, 2H), 2.82−2.63 (m, 6H), 1.81 (s, 3H); ^{13}C NMR ($CDCl_3$) δ 190.7 (s), 165.9 (s), 154.7 (s), 144.2 (s), 131.9 (s), 129.8 (d), 129.0 (d), 128.5 (d), 128.3 (d), 128.1 (d), 126.1 (s), 122.7 (s), 112.2 (d), 107.7 (s), 66.5 (t), 45.1 (t), 35.5 (t), 26.0 (t), 24.7 (t), 10.2 (q); MS *m*/*z* 347 (M^+, 90), 277 (54), 240 (32), 183 (27), 91 (100), 77 (38). Anal. ($C_{22}H_{21}NO_3$) C, H, N.

8-Carboxyphenyl-4-methyl-2,3,5,6,-tetrahydro-(1*H*)-benzo[*c*]quinolizin-3-one (40). Into an autoclave **12** (50 mg, 0.17 mmol), $PdCl_2$ (8 mg, 0.046 mmol), PPh_3 (24 mg, 0.092 mmol), NEt_3 (60 μL, 0.44 mmol), and phenol (500 mg, 5.3 mmol) were mixed with 3.5 mL of benzene. The autoclave was filled with CO (50 bar) and then heated to 120 °C for 24 h. After this period the mixture was cooled to room temperature and the solvent was evaporated under reduced pressure. The residue was dissolved in CH_2Cl_2 (10 mL) and washed with H_2O (2 × 10 mL) and KOH 5% (2 × 10 mL). The organic layer was dried over Na_2SO_4 and after evaporation of the solvent the obtained crude product was chromatographed (EtOAc/petroleum ether 1:1, $R_f = 0.25$), affording pure **40** (50 mg, 88%): mp 183−184 °C; ^{1}H NMR ($CDCl_3$) δ 8.06 (dd, $J_1 = 8.8$ Hz, $J_2 = 2.2$ Hz, 1H), 7.95 (s, 1H), 7.45−7.17 (m, 5H), 7.02 (d, $J = 8.8$ Hz, 1H), 3.99 (t, $J = 7.5$ Hz, 2H), 2.87−2.66 (m, 6H), 1.83 (s, 3H); ^{13}C NMR ($CDCl_3$) δ 190.7 (s), 164.6 (s), 154.4 (s), 150.9 (s), 144.7 (s), 130.4 (d), 129.5 (d), 129.3 (d), 126.3 (s), 125.7 (d), 122.0 (s), 121.6 (d), 112.4 (d), 108.0 (s), 45.2 (t), 35.5 (t), 26.0 (t), 24.8 (t), 10.3 (q); MS *m*/*z* 333 (M^+, 36), 240 (100), 211 (51). Anal. ($C_{21}H_{19}NO_3$) C, H, N.

4-Methyl-2,3,5,6,-tetrahydro-(1*H*)-benzo[*c*]quinolizin-3-one-8-carboxylic Acid *p*-(*tert*-Butyl)phenyl Ester (41). 41 was prepared as reported for **40**, starting from **12** (50 mg, 0.17 mmol) and using *p*-*tert*-butylphenol (510 mg, 3.4 mmol). After chromatography (EtOAc/petroleum ether 1:1, $R_f = 0.29$) pure **41** (46 mg, 70%) was obtained as a white solid: ^{1}H NMR ($CDCl_3$) δ 8.07 (d, $J = 8.8$ Hz, 1H), 7.94 (s, 1H), 7.42 (AB, 2H), 7.10 (AB, 2H), 7.01 (d, $J = 8.8$ Hz, 1H), 3.99 (t, $J = 7.7$ Hz, 2H), 2.87−2.66 (m, 6H), 1.83 (s, 3H), 1.32 (s, 9H); ^{13}C NMR ($CDCl_3$) δ 190.7 (s), 164.7 (s), 154.5 (s), 148.4 (s), 144.5 (s), 131.8 (s), 130.3 (d), 129.4 (d), 126.2 (d), 122.1 (s), 120.8 (d), 112.3 (d), 107.9 (s), 97.8 (s), 45.1 (t), 35.4 (t), 34.4 (s), 31.4 (q), 25.9 (t), 24.7 (t), 10.2 (q); MS *m*/*z* 389 (M^+, 4), 240 (100), 212 (15). Anal. ($C_{25}H_{27}NO_3$) C, H, N.

4-Methyl-2,3,5,6,-tetrahydro-(1*H*)-benzo[*c*]quinolizin-3-one-8-carboxylic Acid *p*-(Carboxymethyl)phenyl Ester (42). 42 was prepared as reported for **40**, starting from **12** (50 mg, 0.17 mmol) and using *p*-caboxymethylphenol (530 mg, 3.5 mmol). After chromatography (EtOAc/petroleum ether 1:1, $R_f = 0.37$) pure **42** (38 mg, 58%) was obtained as a white solid: ^{1}H NMR ($CDCl_3$) δ 8.10 (AB, 2H), 8.03 (d, $J = 8.8$ Hz, 1H), 7.94 (s, 1H), 7.28 (AB, 2H), 7.02 (d, $J = 8.8$ Hz, 1H), 3.99 (t, $J = 7.7$ Hz, 2H), 3.92 (s, 3H), 2.84−2.67 (m, 6H), 1.83 (s, 3H); ^{13}C NMR ($CDCl_3$) δ 190.8 (s), 166.2 (s), 164.1 (s), 154.5 (s), 154.3 (s), 144.9 (s), 131.1 (d), 130.5 (d), 129.6 (d), 127.5 (s), 126.4 (s), 121.7 (d), 121.4 (s), 112.4 (d), 108.2 (s), 52.2 (q), 45.2 (t), 35.5 (t), 25.9 (t), 24.8 (t), 10.3 (q); MS *m*/*z* 391 (M^+, 4), 240 (67), 211 (7), 150 (8), 105 (100), 83 (37); MS *m*/*z* 391 (M^+, 11), 240 (100), 212 (44). Anal. ($C_{23}H_{21}NO_5$) C, H, N.

4-Methyl-2,3,5,6,-tetrahydro-(1*H*)-benzo[*c*]quinolizin-3-one-8-carboxylic Acid *m*-(Carboxymethyl)phenyl Ester (43). 43 was prepared as reported for **40**, starting from **12** (50

mg, 0.17 mmol) and using *m*-caboxymethylphenol (530 mg, 3.5 mmol). After chromatography (CH_2Cl_2/MeOH 40:1, $R_f = 0.32$) pure **43** (47 mg, 71%) was obtained as a white solid: ^{1}H NMR ($CDCl_3$) δ 8.06 (dd, $J_1 = 8.8$ Hz, $J_2 = 2.2$ Hz, 1H), 7.95−7.86 (m, 3H), 7.52−7.38 (m, 2H), 7.02 (d, $J = 8.8$ Hz, 1H), 3.99 (t, $J = 7.7$ Hz, 2H), 3.90 (s, 3H), 2.91−2.67 (m, 6H), 1.83 (s, 3H); ^{13}C NMR ($CDCl_3$) δ 190.7 (s), 166.0 (s), 164.3 (s), 154.3 (s), 150.7 (s), 144.8 (s), 131.5 (s), 130.4 (d), 129.5 (d), 129.3 (d), 126.8 (d), 126.3 (2C, d + s), 122.8 (d), 121.4 (s), 112.4 (d), 108.1 (s), 52.2 (q), 45.1 (t), 35.4 (t), 25.9 (t), 24.7 (t), 10.2 (q); MS *m*/*z* 391 (M^+, 8), 240 (100), 211 (17). Anal. ($C_{23}H_{21}NO_5$) C, H, N.

4-Methyl-2,3,5,6,-tetrahydro-(1*H*)-benzo[*c*]quinolizin-3-one-8-carboxylic Acid *p*-(Methyl)phenyl Ester (44). 44 was prepared as reported for **40**, starting from **12** (50 mg, 0.17 mmol) and using *p*-methylphenol (355 μL, 3.4 mmol). After chromatography (EtOAc/petroleum ether 1:1, $R_f = 0.40$) pure **44** (25 mg, 46%) was obtained as a white solid: ^{1}H NMR ($CDCl_3$) δ 8.05 (d, $J = 8.4$ Hz, 1H), 7.93 (s, 1H), 7.20 (AB, 2H), 7.05 (AB, 2H), 7.01 (d, $J = 8.4$ Hz, 1H), 3.98 (t, $J = 7.4$ Hz, 2H), 2.87−2.66 (m, 6H), 2.35 (s, 3H), 1.83 (s, 3H); ^{13}C NMR ($CDCl_3$) δ 190.8 (s), 164.8 (s), 154.5 (s), 148.6 (s), 144.6 (s), 135.4 (s), 130.4 (d), 129.9 (d), 129.5 (d), 126.3 (s), 122.1 (s), 121.3 (d), 112.3 (d), 108.0 (s), 45.2 (t), 35.5 (t), 26.0 (t), 24.8 (t), 20.9 (q), 10.3 (q); MS *m*/*z* 347 (M^+, 8), 240 (100), 211 (26), 154 (7), 78 (9). Anal. ($C_{22}H_{21}NO_3$) C, H, N.

2. Biology. All compounds were tested according to the procedure already reported.[17a]

3. Molecular Modeling. 3.1. Construction of the Models. The molecular models were built by properly modifying the 19-nor-10-aza-androstenedione skeleton retrieved from the Cambridge Structural Database (CSD code NOVDOR[21]) and by adding the proper fragments from the standard library of SYBYL (Tripos Inc., St. Louis, MO). The models were minimized first by using steepest descent and then conjugate gradient until a convergence of 0.05 kcal mol^{-1} Å^{-1} on the gradient was reached. When needed, conformational searches were carried out, and the minimum energy conformers were optimized by means of the semiempirical Hamiltonian PM3[31] as implemented in the SYBYL graphic interface to MOPAC (keyword PRECISE). The geometry of the conformations chosen for the CoMFA analysis was first optimized at the HF/6-31G* level of theory and eventually at DFT/B3LYP/6-31G* to properly account for the electron correlation effects.

3.2. Conformational Search. For the benzo[*c*]quinolizin-3-one skeleton, the 1α,2β,6α conformation was kept fixed because it was previously determined to be a minimum energy conformation and to better fit onto the well-known 5αR-1 selective inhibitor LY191704 (Figure 1).[17a] The conformational analyses were therefore carried out to sample the rotatable bonds of the substituent at position 8 of the benzo[*c*]quinolizin-3-one skeleton. Since some inhibitors bear a fairly flexible substituent in that position, the conformational space was sampled by means of Monte Carlo analyses[32] using the MMFF force field[33] and the generalized Born/surface area (GB/SA) continuum solvation model[34] for water as implemented in MacroModel software.[35] In a Monte Carlo study, the phase space of a molecule is sampled by randomly changing dihedral angle rotations or atom positions. Then the trial conformation is accepted if its energy has decreased from the previous one. If the energy is higher, various criteria can be applied to accept or reject the Monte Carlo trial. In the present simulations, the number of Monte Carlo steps was set equal to 7000 and the trial conformation was accepted if the energy was lower than that of the previous conformation or if its energy was within an energy window of 100 kJ/mol. Then the conformations were classified by means of a cluster analysis[36] using geometrical parameters as filtering screens.

3.3. Electrostatic Computations. In a CoMFA model, the electrostatic contribution to the final 3D QSAR equation strongly depends on the quality of the point charges. For this reason, we thought to compute the inhibitor charges by means of the RESP procedure,[37] i.e., by fitting them to an electrostatic potential (ESP) calculated at the DFT level using the exchange and correlation functional B3LYP[29] and with the 6-31G* basis set. In detail, the chosen conformations for the CoMFA analysis were first geometrically optimized until a nuclear convergence of 3×10^{-4} on the gradient was reached, and then the ESP was calculated. Finally, by means of the RESP procedure, the atomic partial charges were obtained fitting them on the ESP. The dipole moment was directly obtained as a physical observable from the DFT calculations. All quantum chemical computations were carried out using the Gaussian 98 suite of program (Gaussian 98, Gaussian, Inc., Pittsburgh, PA, 1998).

3.4. 3D QSAR through CoMFA. A 3D QSAR model was obtained by means of the comparative molecular field analysis (CoMFA).[38] The most critical step in the CoMFA procedure is the alignment of the molecules in Cartesian space. In the present work, the 5αR-1 inhibitors were aligned by superimposing atom by atom the benzo[*c*]quinolizin-3-one skeleton of the set of compounds. The molecules bearing a flexible group at position 8 of the benzo[*c*]quinolizin-3-one moiety (**14**−**20**, **35**−**39**, **40**−**42**, and **44**) were aligned by using the *Z* and *E* phenylvinyl derivatives (**22**, **26**) as templates. To this aim, both diastereoisomers were synthesized, and because they present quite different inhibitory potencies (see Table 1), the inhibitors with high biological activity ($pIC_{50} > 6.5$; **14**−**19**, **35**, **36**, **39**, and **42**) were aligned onto the *Z*-**22**, and those with low potency ($pIC_{50} < 6.5$; **20**, **37**, **38**, **40**, **41**, and **44**) were aligned onto the *E* isomer **26**. A CoMFA table was built containing the biological activities of the set of 5αR-1 inhibitors (the dependent variables, pIC_{50obsd} in Table 1) and the values of steric and electrostatic fields at discrete points of the Cartesian space surrounding the molecules (the independent variables). The fields were generated by using an sp^3 carbon atom with a formal charge of +1 as a probe. The region was generated automatically around the molecules by fixing a grid spacing of 2 Å. Moreover, two additional independent variables were taken into account to compute the 3D QSAR equation, i.e., the dipole moment calculated at the DFT level and the log *P* value estimated with the ClogP program[39] (Table 1). The statistical analyses were carried out by applying the PLS procedure to the appropriate variables and using the standard scaling method (COMFA_STD). Furthermore, to reduce the number of independent variables, an energy cutoff value of 30 kcal/mol was selected for both electrostatic and steric fields. The minimum σ for further filtering of the independent variables was set to 2.0 kcal/mol. Cross-validated PLS runs were carried out to establish the optimal number of components (the latent variables) to be used in the final fitting models. The number of cross-validated groups was always equal to the number of compounds (leave-one-out procedure), and the optimal number of latent variables was chosen by considering the lowest standard error of prediction (s_{cross}). All of the independent variables were checked against each other for possible collinearity; no significant cross-correlations were found. In particular, collinearity was not found between the dipole moment and the electrostatic field or between log *P* and the steric field. Finally, scrambling analyses were performed to rule out the possibility of chance correlations.

Acknowledgment. This work was supported by grants from MIUR and Serono International (Geneva, Switzerland). The quantum chemical DFT calculations were carried out on an SGI Origin 3800 machine, taking advantage of a grant provided by the supercomputer center CINECA, Bologna, Italy. Mr. Sandro Papaleo, Mrs. Brunella Innocenti, and Mr. Claudio Piazza are acknowledged for their technical assistance.

Supporting Information Available: Elemental analysis data. This material is available free of charge via the Internet at http://pubs.acs.org.

References

(1) Geller, J. Benign Prostatic Hyperplasia: Pathogenesis and Medical Therapy. *J. Am. Geriatr. Soc.* **1991**, *39*, 1208−1266.

(2) (a) Gormley, G. J. Role of 5α-Reductase Inhibitors in the Treatment of Advanced Prostatic Carcinoma. *Urol. Clin. North Am.* **1991**, *18*, 93−98. (b) Brawley, O. W.; Ford, G. L.; Thompson, I.; Perlman, J. A.; Kramer, B. S. 5α-Reductase Inhibition and Prostate Cancer Prevention. *Cancer Epidemiol., Biomarkers Prev.* **1994**, *3*, 177−182.

(3) Dallob, A. L.; Sadick, N. S.; Unger, W.; Lipert, S.; Geissler, L. A.; Gregoire, S. L.; Nguyen, H. H.; Moore, E. C.; Tanaka, W. K. The Effect of Finasteride, a 5α-Reductase Inhibitor, on Scalp Skin Testosterone and Dihydrotestosterone Concentrations in Patients with Male Pattern Baldness. *J. Clin. Endocrinol. Metab.* **1994**, *79*, 703−706.

(4) Smith, L. S.; Tegler, J. J. Advances in Dermatology. *Annu. Rep. Med. Chem.* **1989**, *24*, 177−186.

(5) (a) Price, V. H. Treatment of Hair Loss. *N. Engl. J. Med.* **1999**, *341*, 964−973 and references therein. (b) Gadwood, R. C.; Fiedler, V. C. Pathogenesis and Treatment of Alopecia. *Annu. Rep. Med. Chem.* **1989**, *24*, 187−196.

(6) Brooks, J. R. Treatment of Hirsutism with 5α-Reductase Inhibitors *Clin. Endocrinol. Metab.* **1986**, *15*, 391−405.

(7) Metcalf, B. W.; Levy, M. A.; Holt, D. A. Inhibitors of Steroid 5α-Reductase in Benign Prostatic Hyperplasia, Male Pattern Baldness and Acne. *Trends Pharmacol. Sci.* **1989**, *10*, 491−495.

(8) (a) Holt, D. A.; Levy, M. A.; Metcalf, B. W. Inhibition of Steroid 5α-Reductase. In *Advances in Medicinal Chemistry*; Maryanoff, B. E., Maryanoff, C. A., Eds.; JAI Press Inc: Greenwich, CT, 1993; Vol. 2, pp 1−29. (b) Abell, A. D.; Henderson, B. R. Steroidal and Non-Steroidal Inhibitors of Steroid 5α-Reductase. *Curr. Med. Chem.* **1995**, *2*, 583−597. (c) Li, X.; Chen, C.; Singh, S.; Labrie, F. The Enzyme and Inhibitors of 4-Ene-3-oxosteroid 5α-Oxidoreductase. *Steroids* **1995**, *60*, 430−441. (d) Frye, S. V. Inhibitors of 5α-Reductase. *Curr. Pharm. Des.* **1996**, *2*, 59−84.

(9) (a) Russell, D. W.; Wilson, J. D. Steroid 5α-Reductases: Two Genes/Two Enzymes. *Annu. Rev. Biochem.* **1994**, *63*, 25−61. (b) Wilson, J. D.; Griffin, J. E.; Russell, D. W. Steroid 5α-Reductase 2 Deficiency. *Endocr. Rev.* **1993**, *14*, 577−593.

(10) Rasmusson, G. H. Chemical Control of Androgen Action. *Annu. Rep. Med. Chem.* **1986**, *22*, 179−188.

(11) (a) Imperato-McGinley, J.; Guerrero, L.; Gautier, T.; Peterson, R. E. Steroid 5α-reductase deficiency in man: an inherited form of male pseudohermaphroditism. *Science* **1974**, *186*, 1213. (b) Jenkins, E. P.; Andersson, S.; Imperato-McGinley, J.; Wilson, J. D.; Russell, D. W. Genetic and pharmacological evidence for more than one human steroid 5 alpha-reductase *J. Clin. Invest.* **1992**, *89*, 293.

(12) Jones, C. D.; Audia, J. E.; Lawhorn, D. E.; McQuaid, L. A.; Neubauer, B. L.; Pike, A. J.; Pennington, P. A.; Stamm, N. A.; Toomey, R. E.; Hirsch, K. R. Nonsteroidal Inhibitors of Human Type I Steroid 5α-Reductase. *J. Med. Chem.* **1993**, *36*, 421−423

(13) Wikel, J. H.; Bemis, K. G.; Audia, J. E.; McQuaid, L. A.; Jones, C. D.; Pennington, P. A.; Lawhorn, D. E.; Hirsch, K. R.; Stamm, N. B. QSAR Study of Benzoquinolinones as Inhibitors of Human Type 5α-Reductase. *Bioorg. Med. Chem. Lett.* **1993**, *3*, 1157−1162.

(14) Abell, A. D.; Erhard, K. F.; Yen, H.-K.; Yamashita, D. S.; Brandt, M.; Mohammed, H.; Levy, M. A.; Holt, D. A. Preparative Chiral HPLC Separation of all Possible Stereoisomers of LY191704 and LY266111 and Their in Vitro Inhibition of Human Types 1 and 2 Steroid 5α-Reductase. *Bioorg. Med. Chem. Lett.* **1994**, *4*, 1365.

(15) Smith, E. C. R.; McQuaid, L. A.; Goode, R. L.; McNulty, A. M.; Neubauer, B. L.; Rocco, V. P.; Audia, J. E. Synthesis and 5α-Reductase Inhibitory Activity of 8-Substituted Benzo[*f*]quinolinones Derived from Palladium Mediated Coupling Reactions. *Bioorg. Med. Chem. Lett.* **1998**, *8*, 395−398.

(16) Abell, A. D.; Brandt, M.; Levy, M. A.; Holt, D. A. A Comparison of Steroidal and Nonsteroidal Inhibitors of Human Steroid 5a-Reductase: New Tricyclic Aryl Acid Inhibitors of the Type-1 Isozyme. *Bioorg. Med. Chem. Lett.* **1996**, *6*, 481−484.

(17) (a) Guarna, A.; Machetti, F.; Occhiato, E. G.; Scarpi, D.; Comerci, A.; Danza, G.; Mancina, R.; Serio, M.; Hardy, K. Benzo[*c*]-quinolizin-3-ones: A Novel Class of Potent and Selective Non-steroidal Inhibitors of Human Steroid 5α-Reductase 1. *J. Med. Chem.* **2000**, *43*, 3718−3735. (b) Guarna, A.; Occhiato, E. G.; Scarpi, D.; Tsai, R.; Danza, G.; Comerci, A.; Mancina, R.; Serio, M. Synthesis of Benzo[*c*]quinolizin-3-ones: Selective Non-Steroidal Inhibitors of Steroid 5α-Reductase 1. *Bioorg. Med. Chem. Lett.* **1998**, *8*, 2871−2876. (c) Guarna, A.; Occhiato, E. G.; Scarpi, D.; Zorn, C.; Danza, G.; Comerci, A.; Mancina, R.; Serio, M. Synthesis of 8-Chloro-benzo[*c*]quinolizin-3-ones as Potent and Selective Inhibitors of Human Steroid 5α-Reductase 1. *Bioorg. Med. Chem. Lett.* **2000**, *10*, 353.

(18) Thiboutot, D.; Harris, G.; Iles, V.; Cimis, G.; Gilliland, K.; Hagari, S.; Activity of the Type 1 5α-Reductase Exhibits Regional Differences in Isolated Sebaceous Glands and Whole Skin. *J. Invest. Dermatol.* **1995**, *105*, 209−214.

(19) (a) Kenny, B.; Ballard, S.; Blagg, J.; Fox, D. Pharmacological Options in the Treatment of Benign Prostatic Hyperplasia. *J. Med. Chem.* **1997**, *40*, 1293−1314. (b) Harris, G. S.; Kozarich, J. W. Steroid 5α-Reductase Inhibitors in Androgen-Dependent Disorders. *Curr. Opin. Chem. Biol.* **1997**, *1*, 254−259.

(20) Guarna, A.; Belle, C.; Machetti, F.; Occhiato, E. G.; Payne, H. P.; Cassiani, C.; Comerci, A.; Danza, G.; De Bellis, A.; Dini, S.; Marrucci, A.; Serio, M. 19-Nor-10-azasteroids: A Novel Class of Inhibitors for Human Steroid 5α-Reductases 1 and 2. *J. Med. Chem.* **1997**, *40*, 1112−1129.

(21) Guarna, A.; Occhiato, E. G.; Machetti, F.; Marrucci, A.; Danza, G.; Serio, M.; Paoli, P. 19-Nor-10-azasteroids, a New Class of Steroid 5α-Reductase Inhibitors. 2. X-ray Structure, Molecular Modeling, Conformational Analysis of 19-Nor-10-azasteroids and Comparison with 4-Azasteroids and 6-Azasteroids. *J. Med. Chem.* **1997**, *40*, 3466−3477.

(22) (a) Cavalli, A., Ed. Density functional theory. *Quant. Struct.−Act. Relat.* **2002**, *21*. (b) Carloni, P.; Alber, F. Quantum Medicinal Chemistry. In *Methods and Principles in Medicinal Chemistry*; Mannhold, R., Kubinyi, H., Folkers, G., Eds.; Wiley-VCH: Weinheim, Germany, 2003.

(23) Guarna, A.; Lombardi, E.; Machetti, F.; Occhiato, E. G.; Scarpi, D. Modification of the aza-Robinson Annulation for the Synthesis of 4-Methyl-benzo[*c*]quinolizin-3-ones, Potent Inhibitors of Steroid 5α-Reductase 1. *J. Org. Chem.* **2000**, *65*, 8093−8095

(24) All new compounds were also tested with human recombinant 5αR-2 isozyme expressed in CHO 1829, some of them displaying activity toward this isozyme.

(25) Thigpen, A. E.; Cala, K. M.; Russel, D. W. Characterization of Chinese Hamster Ovary Cell Lines Expressing Human Steroid 5α-Reductase Isozymes. *J. Biol. Chem.* **1993**, *268*, 17404−17412.

(26) Program kindly furnished by the following: De Lean, A.; Munson, P. J.; Guardabasso, V.; Rodbard, D.; Laboratory of Theoretical and Physical Biology, National Institute of Child Health and Human Development, National Institutes of Health, Bethesda, MD 20892.

(27) (a) Tian, G.; Stuart, J. D.; Moss, M. L.; Domanico, P. L.; Bramson, H. N.; Patel, I. R.; Kadwell, S. H.; Overton, L. K.; Kost, T. A.; Mook, R. A., Jr.; Frye, S. V.; Batchelor, W. K.; Wiseman, J. S. 17*β*-(N-*tert*-butylcarbamoyl)-4-aza-5α-androstan-1-en-3-one is an active site-directed slow time-dependent inhibitor of human steroid 5α-reductase 1. *Biochemistry* **1994**, *33*, 2291−2296. (b) Bull, H. G.; Garcia-Calvo, M.; Anderson, S.; Baginsky, W. S.; Chan, H. K.; Ellsworth, D. E.; Miller, R. R.; Stearns, R. A.; Bakshi, R. K.; Rasmusson, G. H.; Tolman, R. L.; Myers, R. W.; Kozarich, J. W.; Harris, G. S. Mechanism-based inhibition of human steroid 5α-reductase by finasteride: enzyme-catalyzed formation of NADP-dihydrofinasteride, a potent bisubstrate analog inhibitor. *J. Am. Chem. Soc.* **1996**, *118*, 2359−2365.

(28) Guarna, A.; Occhiato, E. G.; Machetti, F.; Trabocchi, A.; Scarpi, D.; Danza, G.; Mancina, R.; Comerci, A.; Serio, M. Effect of C-Ring Modifications in Benzo[*c*]quinolizin-3-ones, New Selective Inhibitors of Human 5α-Reductase 1. *Bioorg. Med. Chem.* **2001**, 9, 1385−1393.

(29) Becke, A. D. A new mixing of Hartree−Fock and local density-functional theories. *J. Chem. Phys.* **1993**, *98*, 1372−1377.

(30) Sulpizi, M.; Schelling, P.; Folkers, G.; Carloni, P.; Scapozza, L. The rational of catalytic activity of herpes simplex virus thymidine kinase. a combined biochemical and quantum chemical study. *J. Biol. Chem.* **2001**, *276*, 21692−21697.

(31) Stewart, J. P. P. Optimization of parameters for semiempirical methods I. Method. *J. Comput. Chem.* **1989**, *10*, 209−220.

(32) Chang, G.; Guida, W. C.; Still, W. C. An internal coordinate Monte Carlo method for searching conformational space. *J. Am. Chem. Soc.* **1989**, *111*, 4379−4386.

(33) Halgren, T. A. Merck molecular force field. I. Basis, form, scope, parameterization, and performance of MMFF94. *J. Comput. Chem.* **1996**, *17*, 490−519.

(34) Still, W. C.; Tempzyk, A.; Hawley, R.; Hendrickson, T. Semianalytical treatment of solvation for molecular mechanics and dynamics. *J. Am. Chem. Soc.* **1990**, *112*, 6127−6129.

(35) Mohamadi, F.; Richards, N. G. J.; Guida, W. C.; Liskamp, R. M. J.; Lipton, M. A.; Caulfield, C. E.; Chang, G.; Hendrickson, T. F.; Still, W. C. MacroModel−an integrated software system for modeling organic and bioorganic molecules using molecular mechanics. *J. Comput. Chem.* **1990**, *1*, 440−467.

(36) Shenkin, P. S.; McDonald, D. Q. Cluster analysis of molecular conformations. *J. Comput. Chem.* **1994**, *15*, 899−916.

(37) Bayly, C. I.; Cieplak, P.; Cornell, W. D.; Kollman, P. A. A well-behaved electrostatic potential based method using charge restraints for determining atom-centered charges: the RESP model. *J. Phys. Chem.* **1993**, *97*, 10269−10280.

(38) Cramer, R. D.; Patterson, D. E.; Bunce, J. D. Comparative molecular field analysis (CoMFA). 1. Effect of shape on binding of steroids to carrier proteins. *J. Am. Chem. Soc.* **1988**, *110*, 5959−5967.
(39) *ClogP*, version 4.3; BioByte Corp.: Claremont, CA.
(40) The r^2_{pred} was evaluated by solving the equation $r^2_{pred} = (SD - PRESS)/SD$, where SD is the sum of the squared deviations of each observed activity value for each molecule of the test set from the mean of the observed activity values of the training set (pIC_{50obsd} values of Table 1) and where PRESS is the sum of the squared deviations between predicted and observed values (Δ of Table 3).

JM031131O